Hydrophobic Forces in Wetting Films

Lei Pan

Thesis submitted to the Faculty of the
Virginia Polytechnic Institute and State University
in partial fulfillment of the requirement for the degree of

Master of Science

in

Mining and Minerals Engineering

Dr. Roe-Hoan Yoon, Chairman
Dr. Gregory T. Adel
Dr. Gerald H. Luttrell

December 7, 2009

Blacksburg, Virginia

Keywords: hydrophobic forces, wetting film, thinning kinetics, combining rule

Copyright © 2009 by Lei Pan

Hydrophobic Forces in Wetting Films

Lei Pan

Abstract

Flotation is an important separation process used in the mining industry. The process is based on hydrophobizing a selected mineral using an appropriate surfactant, so that an air bubble can spontaneously adhere on the mineral surface. The bubble-particle adhesion is possible only when the thin film of water between the bubble and particle ruptures, just like when two colloidal particles or air bubbles adhere with each other. Under most flotation conditions, however, both the double-layer and dispersion forces are repulsive, which makes it difficult to model the rupture of the wetting films using the DLVO theory.

In the present work, we have measured the kinetics of film thinning between air bubble and flat surfaces of gold and silica. The former was hydrophobized by *ex-site* potassium amyl xanthate, while the latter by *in-site* Octadecyltrimetylammonium chlroride. The kinetics curves obtained with and without theses hydrophobizing agents were fitted to the Reynolds lubrication theory by assuming that the driving force for film thinning was the sum of capillary pressure and the disjoining pressure in a thin film. It was found that the kinetics curves obtained with hydrophilic surfaces can be fitted to the theory with the disjoining pressure calculated from the DLVO theory. With hydrophobized surfaces, however, the kinetics curves can be fitted only by assuming the presence of a non-DLVO attractive force (or hydrophobic force) in the wetting films. The results obtained in the present work shows that long-range hydrophobic forces is responsible for the faster drainage of wetting film.

It is shown that the changes in hydrophobic forces upon the thin water film between air bubble and hydrophobic surface is dependent on hydrophobizing agent concentration, immersion time and the electrolyte concentration in solution. The obtained hydrophobic forces constant in wetting film K_{132} is compared with the hydrophobic forces constant between two solid surfaces K_{131} to verify the combining rule for flotation.

Acknowledgement

First and foremost, I would like to acknowledge my advisor, Dr. Roe-Hoan Yoon, for his support and guidance throughout my first one and half year study in Virginia Tech. I would like to express my appreciation to him for his sincere suggestion on my research life and his care on my personal life in Blacksburg. During this period, I have learned a lot from Dr. Yoon about how to conduct research projects, how to think, how to write. I also thank Dr. Gregory Adel and Dr. Gerald Luttrell who served as my thesis committee member for their suggestions on my research works.

I sincerely appreciate to Ruijia Wang for his instruction and training on thin film balance technique, and Dr. Jialin Wang for his guidance and instruction in preparing the hydrophobic surface in our lab. Especially, I would like to thank Mr. Zuoli Li who measured the hydrophobic forces between gold surfaces in pure water for me to verify the combining rule.

I would like to express my appreciation to Hyunsun Do for his discussion on theoretical model of wetting film drainage. Also I want to express my sincere gratitude to Dr. Liguang Wang for his discussion on thinning kinetics and TFB technique.

I would like to thank past and present members in Center of Advanced Separation Techniques (CAST), Charles Schlosser, Chad Freeland for their discussion and friendship, Chris Hull, Kathy Flint, Dongcheol Shin and Dr. Jinming Zhang for their support and help.

Last but not least, I would like to express my deepest gratitude to my parents for their selfless love and support. Without their love and support, I would not have my accomplishment.

Tables of Contents

List of Figures

List of Tables

Chapter 1

Introduction

1.1 General

Froth flotation has been widely used in industry for more than 100 years to separate the different minerals from each other, ever since the gas bubble was first recognized as a means of mineral separation by Bassel brothers in Germany in 1886.[1, 2] Even today after 100 years since its commercial inception in 1905, froth flotation is still the most successful and cheapest technique in many separating industry, such as deinking[3-5], oil recovery from oil sand[6-8], and coal cleaning[9-11]. The basic principle of froth flotation is rendering the target mineral hydrophobic using appropriate surfactants and untarget mineral hydrophilic. The gas bubbles prefer to attach the hydrophobic particles, and rise to the top of cell, forming the three-phase froth. The attachment between the gas bubble and the particle is the fundamental process for flotation. As described in previous literatures[12], the initial approach of gas bubbles to the particles is controlled by turbulent flow generated by the agitator. As the intervening water layers between the gas bubble and the particle become thinner, the surface forces become an active component to control the thinning and rupture of the water thin film between the gas bubble and particle which is usually titled "wetting film" in colloidal science. On the hydrophobic surface, the wetting film will spontaneously rupture forming the three-phase froth. Recognizing the significance of the interaction between the gas bubble and the particle related to the flotation condition, many investigators tried to better understand the interaction energy between air bubbles and particles in order to predict the flotation behavior and improve the flotation cell design.

The DLVO theory was named after Derjaguin and Landau[13], Verwey and Overbeek[14], two independent research groups who first formulated the classical standard theory of colloidal dispersions that comprised both the repulsion and attraction forces. Classical DLVO theory contains two additive components: van der Waals dispersion energy (V_d) and electrostatic double layer energy (V_e). Thus the total interaction energy could be represented as follows:

$$V_t = V_d + V_e \qquad [1.1]$$

For interaction between spherical gas bubble and spherical particle of radii R_1 and R_2, the dispersion energy (V_d) is described by the following expression

$$V_d = -\frac{A_{132}R_1R_2}{6H(R_1+R_2)}\left[1-\frac{1+2bl}{1+bc/H}\right] \qquad [1.2]$$

where A_{132} is the Hamaker constant of particle (1) and bubble (2) interaction in the aqueous medium (3), and H is the separation distance. The second part of the equation represents the correction factor due to the retardation effect in presence of the electrolyte in solution. Since the Hamaker constant of water (A_{33}) is less than that of the solid (A_{11}) but greater than that of the air (A_{22}), A_{132} is negative according to the combining rule[15]. Thereby, the dispersion energy between the gas bubble and the particle is always repulsive.

The interaction energy due to the overlapping electrostatic double layers could be represented using the HHF's expression[16]

$$V_e = \frac{\varepsilon R_1 R_2(\psi_1^2+\psi_2^2)}{4(R_1+R_2)}\left[\frac{2\psi_1\psi_2}{\psi_1^2+\psi_2^2}\ln\left(\frac{1+e^{-\kappa h}}{1-e^{-\kappa h}}\right)+\ln\left(1-e^{-2\kappa h}\right)\right] \quad [1.3]$$

where ε is the dielectric constant of medium 2, ψ_1 and ψ_2 are the stern potential of the air bubble and the particle and κ^{-1} is referred to as the Debye length.

Under most flotation conditions, both the van der Waals dispersion forces and electrostatic double layer forces are repulsive. According to the classical DLVO theory, the flotation could not happen due to the strong repulsive forces between the gas bubble and particle. It was not utill 1968 that Laskowski and Kitchener[17] found that the water films of a certain thickness on the methylated silica surface were unstable and the wetting film would rupture spontaneously, while both double-layer and dispersion forces were repulsive. Blake and Kitchener[18] later found that the rupture thickness of wetting film on methylated silica was 60 to 220 nm, which indicated that the thin water film on methylated silica was unstable because of presence of "long-range" attractive forces. More recently, Israelachvili and Pashley[19, 20] firstly measured the long-range attractive forces (or hydrophobic forces) between two macroscopic surfaces in CTAB solution using Surface Forces Apparatus (SFA). Other investigators[21-26] also confirmed that there existed the attractive hydrophobic forces between two hydrophobic surfaces using Atomic Force Microscope (AFM) or thin film balance (TFB). Thereby, the DLVO theory must be extended to include a third term for interaction between two macroscopic surfaces, named as "hydrophobic forces"

$$V_t = V_d + V_e + V_h \quad [1.4]$$

where V_h represents the hydrophobic term of interaction energy.

The interaction energy contributed from the hydrophobic forces is usually represented as the exponential function form, as reported in many previous literatures[22, 27]. Therefore, the hydrophobic forces term of interaction energy is represented as follows:

$$V_h = \frac{R_1 R_2}{R_1+R_2}\left[C_1\exp\left(-\frac{H}{D_1}\right)+C_2\exp\left(-\frac{H}{D_2}\right)\right] \quad [1.5]$$

where $C_1\exp\left(-\frac{H}{D_1}\right)$ term represents the short-range hydrophobic forces, the second term represents the long-range hydrophobic forces, *C* represents the magnitude of hydrophobic forces and *D* represents the decay length.

Yoon et al[23, 28] also suggests the hydrophobic forces could be represented as a power law:

$$V_h = -\frac{R_1 R_2}{R_1+R_2}\frac{K_{132}}{6H} \quad [1.6]$$

where K_{132} is the hydrophobic forces constant which is in the same form as that for the nonretarded van der Waals interaction. Thereby, it is easy to compare the hydrophobic forces with van der Waals dispersion forces.

The objective of the present work is to measure thinning kinetics of wetting film between the gas bubble and the hydrophobic plate. Also the combining rule for the hydrophobic forces constant is discussed based on the results obtained in the present work and previous literatures.

1.2 Literature Review

1.2.1 Thermodynamics of Bubble-Particle Contact

Bubble-particle contact is one of the primary factors controlling the flotation process. To minimize the Gibbs free energy, the liquid drop or gas bubble forms a finite contact angle on a smooth solid surface, called three-phase contact, as shown in Fig 1.1. Thermodynamically, the condition for three-phase contact is given by Young's equation.[29, 30]

$$\gamma_{SG} = \gamma_{SL} + \gamma_{LG}\cos\theta \qquad [1.7]$$

where γ_{SG}, γ_{SL} and γ_{LG} are the interfacial tensions of the solid-gas, solid-liquid, liquid-gas interfaces respectively, and θ is the contact angle.

As the gas bubble attaches the solids, the change in the free energy due to the replacement of the solid-liquid interface by solid-gas interface is given by Dupre's equation.

$$\Delta G = \gamma_{SG} - (\gamma_{SL} + \gamma_{LG}) \qquad [1.8]$$

Substituting $\gamma_{SL} - \gamma_{LG}$ term in equation [1.8] using the Young's equation [1.7], the change in free energy could be simplified to the equation as follows

$$\Delta G = \gamma_{LG}(\cos\theta - 1) \qquad [1.9]$$

Thereby the change in free energy is dependent on the interfacial tension (γ_{LG}) at liquid-gas interface and contact angle (θ). The larger the degree of contact angle is and the larger the value of interfacial tension is, the more likely the bubble attaches to the particle. For any finite value of the contact angle, the free energy will always decrease upon the attachment of the gas bubble to the particles. This explains why the gas bubble could form a three-phase contact on the solid surface with a finite value of contact angle.

Equation [1.9] is well known as the criteria for possibility of a bubble-particle contact in a liquid medium. However, it is predicted by the equation [1.9] that the gas bubble could attach the solid once the contact angle is above zero, which is conflict with the condition in real flotation practice. The reason behind is that the equation ignores the effect from the thin liquid layer between the air bubble and solid before and after the attachment.

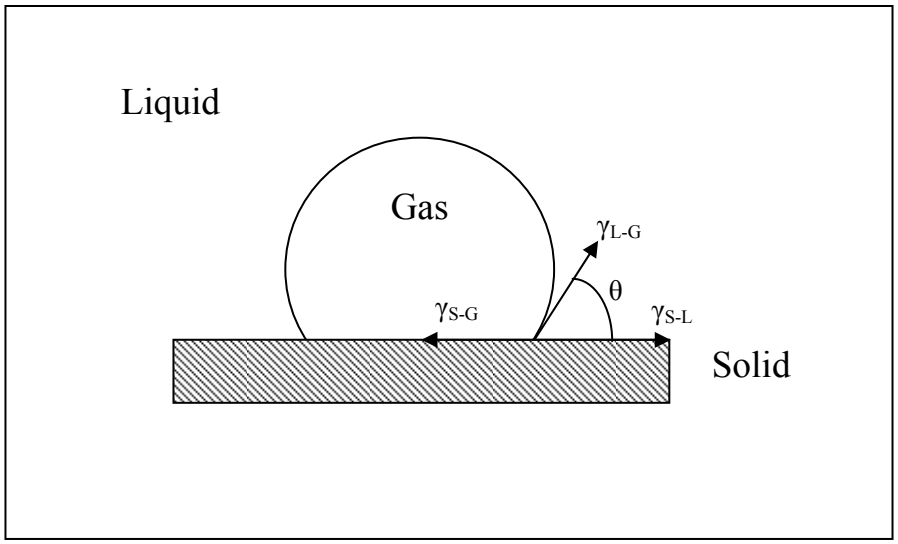

Figure 1.1 Schematic diagram of the gas bubble on a flat solid surface in a liquid medium

Derjaguin et al.[31] first introduced "disjoining pressure" (Π) to define the excess pressure acting on the thin liquid layer from those on the bulk phase. At constant temperature and pressure, the thin liquid film obeys the following thermodynamic fundamental equation,

$$-d\gamma^f = \Gamma_s^{f,ex} d\mu_s + \Pi dh \qquad [1.10]$$

where γ^f is defined as film surface tension, $\Gamma_s^{f,ex}$ denotes the surface excess of film, and μ_s is defined as surface chemical potential. At constant chemical potential, the disjoining pressure Π is represented as follows from equation [1.10][32]

$$\left(\frac{\partial \gamma^f}{\partial h}\right)_{T,P,\mu_s} = -\Pi \qquad [1.11]$$

Therefore, if the film tension (γ^f) decreases as film thickness (h) decreases, the disjoining pressure (Π) will be positive, which is characterized by an attractive disjoining pressure.

1.2.2 Film Thinning in Wetting Film

The properties of thin liquid film between two interfaces are of primary importance for the behavior of the dispersion system. The wetting film is the thin liquid layer sandwiched by a gas-liquid interface and a solid-liquid interface. When a gas bubble approaches a flat solid surface, the "dimpled" shape of wetting film was observed in previous work[33-36] as shown in

Fig 1.2. The "dimpled" shape means that the film thickness at the center is larger than that at its periphery. Thus once a "dimple" is formed, the liquid inside dimple is entrapped by a thinner "barrier ring". Fisher et al.[37] explained that the "dimple" phenomenon is due to viscous liquid drag. The liquid at the barrier ring drains faster than those at the center, and thereby a convex "dimpled" shape is formed. Also the convex shape introduces the positive Laplace pressure that resists the drainage of the liquid inside the dimple.

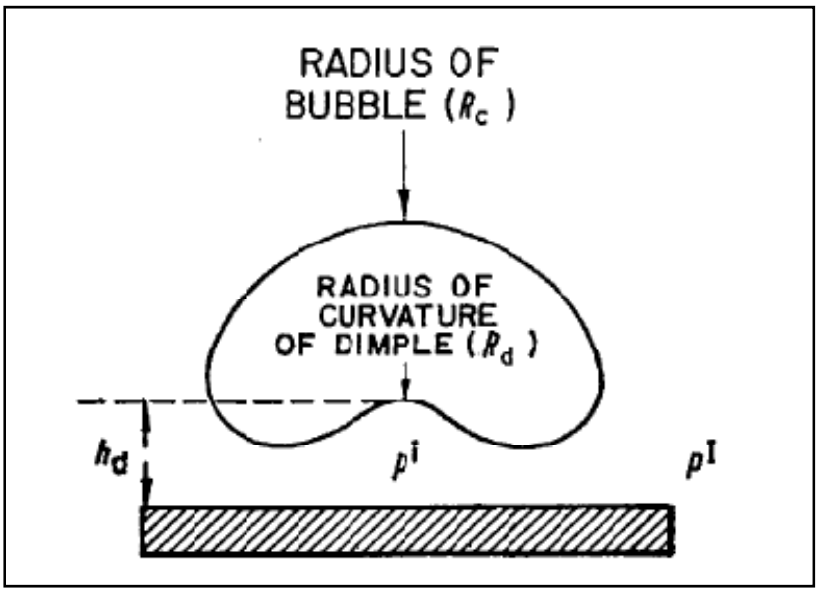

Figure 1.2 Schematic diagram of a "dimple" formation as the gas bubble approaches the flat solid surface[38]

Scheludko[39] first derived an expression as follows to predict the rate of thinning of the film using Reynolds equation, based on the assumption that thin liquid films are plane-parallel.

$$V_{re} = \frac{-dh}{dt} = \frac{2h^3 \Delta P}{3\eta R^2} \qquad [1.12]$$

where R is the radius of the film, η is the viscosity of liquid and ΔP is the driving pressure for film thinning. In Scheludko's cell, the driving pressure ΔP is a sum of the capillary pressure P_σ and disjoining pressure Π. Thus the equilibrium film thickness could be predicted at a finite film thickness where the capillary pressure equates to disjoining pressure.

The derivation of equation 1.12 is based on Reynolds lubrication approximation which assumes that the liquid flows between plane parallel surfaces and the film surfaces are tangentially immobile. Frankel and Mysels[35] developed a purely hydrodynamic theory of the evolution of dimples, assuming that the rate of flow through the barrier ring was independent of the radius. They proposed that the film thickness at the center of dimple h_o and film thickness at the barrier ring h_b as a function of time t is given by Equation [1.13] and Equation [1.14].

$$h_0 = \left(\frac{0.0096 r_0^6 \eta n^2}{\gamma R t}\right)^{1/4} \quad [1.13]$$

$$h_b = \left(\frac{0.006 n^2 R^5 \rho g \eta}{\gamma^t t}\right)^{1/2} \quad [1.14]$$

Frankel-Mysels model is corresponding to experimental observation done by Platikanov[34], but slightly overestimates the "dimple" shape.

After Frankel-Mysels' initial work on the theoretical modeling of draining dimpled film, numerous investigators have developed models describing the thinning of dimpled films. Hartland and Robinson[40] presented a model for an axisymmetric dimpled draining film assuming the film was parabolic. They suggested that pressure is constant at the center of film and falls to zero just outside the barrier ring. Dimitrov and Ivanov[41] derived an equation for the rate of thinning of dimpled films by matching the asymptotic coordinate expansions. It is shown that the film could be considered as practically plane-parallel at a short film thickness. Jain and Ivanov[38] later presented a simplified model for the thinning of dimpled films, assuming that all the energy dissipation takes places in the barrier. They suggested that the presence of a dimple increases the velocity of thinning. Lin and Slattery[42] developed a hydrodynamic model for drainage of thin liquid film which agrees with the experimental results. Also, they suggested that the surface viscosities have little effect upon the drainage rate in presence of surfactants. Chen and Slattery[43, 44] later extended the model for drainage of film by considering the van der Waals forces and electrostatic double-layer forces. Recently, Ralson et al.[45, 46] studied the drainage of aqueous thin film as the gas bubble approach the flat solid surface using scanning interferometry. The experimental equilibrium film thickness agrees with the theoretical prediction by the DLVO theory.

1.2.3 Bubble-Solid Interaction

The colloidal interaction between air bubble and particle was studied for decades by TFB[47], SFA[48, 49] and AFM[50, 51], primarily because it is of utmost importance for flotation. It is well known that the wetting film is stabilized on the hydrophilic surface and ruptures spontaneously on hydrophobic surfaces. Tchaliovska et al.[52] studied the interaction between air bubble and a mica surface immersed in dodecylammonium chloride (DAC) solution. The results showed that hydrophobic attraction forces played a vital role in thin-film lifetimes and rates of expansion of the meniscus perimeter. Yoon and Yordan[53] measured the critical thickness of film on hydrophobic surfaces by using TFB technique. It was shown that critical rupture thickness increases with an increasing degree of methylation. The rupture thickness also reaches the maximum, when pH of the amine solution is 9-9.5 where the adsorption is most favored. The following papers[23, 54-56] by Yoon et al. suggested that thinning and rupture of thin water film intervened by hydrophobic surfaces must include the influence of hydrophobic attractive forces.

The mechanism of attachment between air bubble and hydrophobic particle, however, is still discussed to illustrate the existence of so called "hydrophobic forces". Alexandrova et al.[57]

studied the stability of an aqueous thin film containing tetradecyltrimethylammonium bromide (C_{14}TAB) between air bubbles and silica substrates. They explained that the spontaneous rupture of thin aqueous film was interpreted in terms of electrostatic mechanism, also named as "Heterocoagulation mechanism". At relatively low surfactant concentration, the gas/liquid interface was net positive charged while the liquid/solid interface remained negative charged, which led to an attractive electrostatic forces between gas bubble and solid.

Schulze et al.,[58, 59] suggested that gas bubble at heterogeneous solid surfaces was responsible for the rupture of wetting film on methylated silica without considering any long-range hydrophobic attraction. Mahnke et al.[60] observed a hole in the dimpled wetting film on hydrophobic glass surfaces coated with fatty acid Langmuir-Blodgett layers, and they indicated that nucleation of the air bubble is the reason for the high rupture thickness for hydrophobic surface coated with L-B layers. In other communication, Mahnke et al.,[61] also suggested that the rupture of thin wetting films on methylated glass surfaces was explained by hole formation. Stckelhuber et al.,[62, 63]recently proposed that nanobubbles on the hydrophobic solid surface could be the cause of rupture of wetting films without considering any surface forces acting on the interface.

Vinogradova[64-67] proposed that the observed long-range hydrophobic forces measured in drainage technique may occur due to slippage. It is a possibility that application of Reynolds equation theory may led to overestimating the hydrophobic forces. Thereby, the magnitude of hydrophobic forces correlated to slip lengths of liquid over solid or vapor, which is probably linked to a decrease in viscosity in the vicinity of a solid.

1.3 Research Objective

The objective of present work is to measure the thinning kinetics of wetting film between the gas bubble and the hydrophobic solid surface by Thin Film Balance technique. The hydrophobic forces constant K_{132} is calculated using the Reynolds equation, assuming that Reynolds equation could apply to predict the thinning kinetics of thin water film at the "barrier ring". The obtained K_{132} in wetting film on the hydrophobic surface is used to compare with surface forces data reported in previous literature to determine the validity of the combining rule.

Chapter 2 discusses the drainage of wetting film on the gold surface treated by potassium amyl xanthate (PAX). Chapter 3 describes the drainage of wetting film on the polished quartz surface in octadecyltrimethylammonium chloride (C_{18}TACl) solution.

1.4 References

1. Fuerstenau, D. W., A Century of Developments in the Chemistry of Flotation processing. In *Froth flotation: a century of innovation*, M.C. Fuerstenau, G. J., Roe-Hoan Yoon, Ed. SME: 2007.
2. A.J. Lynch, J. S. W., J.A. Finch, G.E. Harbort, History of Flotation Technology. In *Froth flotation: a century of innovation*, M.C. Fuerstenau, G. J., Roe-Hoan Yoon, Ed. SME: 2007.

3. Liu, J.; Vandenberghe, J.; Masliyah, J.; Xu, Z.; Yordan, J., Fundamental study on talc-ink adhesion for talc-assisted flotation deinking of wastepaper. *Minerals Engineering* **2007,** 20, (6), 566-573.
4. Finch, J. A.; Hardie, C. A., An example of innovation from the waste management industry: Deinking flotation cells. *Minerals Engineering* **1999,** 12, (5), 467-475.
5. Rubio, J.; Souza, M. L.; Smith, R. W., Overview of flotation as a wastewater treatment technique. *Minerals Engineering* **2002,** 15, (3), 139-155.
6. Liu, J.; Xu, Z.; Masliyah, J., Processability of Oil Sand Ores in Alberta. *Energy & Fuels* **2005,** 19, (5), 2056-2063.
7. Goual, L.; Horvath-Szabo, G.; Masliyah, J. H.; Xu, Z., Characterization of the Charge Carriers in Bitumen. *Energy & Fuels* **2006,** 20, (5), 2099-2108.
8. Gu, G.; Zhang, L.; Xu, Z.; Masliyah, J., Novel Bitumen Froth Cleaning Device and Rag Layer Characterization. *Energy & Fuels* **2007,** 21, (6), 3462-3468.
9. Laskowski, J. S., *Coal Flotation and Fine Coal Utilization*. Elsevier: 2001.
10. Borchardt John, K., Chemistry of Unit Operations in Paper Deinking Mills. In *Plastics, Rubber, and Paper Recycling*, American Chemical Society: Washington, DC, 2009; pp 323-341.
11. Borchardt John, K., Deinking of Papers Printed with Water-Based Inks: An Overview. In *Surfactant-Based Separations*, American Chemical Society: Washington, DC, 2009; pp 384-419.
12. Booth, R. B.; Freyberger, W. L., Froth and Frothing Agents. In *Froth Flotation, 50th Anniversary Volume. AIME*, Fuerstenau, D. W., Ed. AIME: New York, 1962; pp 258–276.
13. Landau, B. D. L., Theory of the stability of strongly charged lyophobic sols and of the adhesion of strongly charged particles in solutions of electrolytes. *Acta Physico chemica URSS* **1941,** 14.
14. Verwey EJW, O. J., Theory of the stability of lyophobic colloids, Elsevier, Amsterdam (1948).
15. Israelachvili, J., *Intermolecular & Surface Forces, 2nd Edition*. Academic Press INC.: San Diego, 1992.
16. Hogg, R.; Healy, T. W.; Fuerstenau, D. W., Mutual coagulation of colloidal dispersions. *Trans. Faraday Soc.* **1965,** 62, 14.
17. Laskowski, J.; Kitchener, J. A., The hydrophilic--hydrophobic transition on silica. *Journal of Colloid and Interface Science* **1969,** 29, (4), 670-679.
18. Blake, T. D.; Kitchener, J. A., Stability of aqueous films on hydrophobic methylated silica. *J. Chem. Soc., Faraday Trans. 1* **1972,** 68, 8.
19. Pashley, R. M.; Israelachvili, J. N., A comparison of surface forces and interfacial properties of mica in purified surfactant solutions. *Colloids and Surfaces* **1981,** 2, (2), 169-187.
20. Israelachvili, J.; Pashley, R., The Hydrophobic Interaction Is Long-Range, Decaying Exponentially with Distance. *Nature* **1982,** 300, (5890), 341-342.
21. Wang, J.; Yoon, R.-H., AFM Forces Measured between Gold Surfaces Coated with Self-Assembled Monolayers of 1-Hexadecanethiol. *Langmuir* **2008,** 24, (15), 7889-7896.
22. Yoon, R. H.; Ravishankar, S. A., Long-range hydrophobic forces between mica surfaces in dodecylammonium chloride solutions in the presence of dodecanol. *Journal of Colloid and Interface Science* **1996,** 179, (2), 391-402.
23. Yoon, R. H.; Flinn, D. H.; Rabinovich, Y. I., Hydrophobic interactions between dissimilar surfaces. *Journal of Colloid and Interface Science* **1997,** 185, (2), 363-370.
24. Angarska, J. K.; Dimitrova, B. S.; Danov, K. D.; Kralchevsky, P. A.; Ananthapadmanabhan, K. P.; Lips, A., Detection of the hydrophobic surface force in foam films by measurements of the critical thickness of the film rupture. *Langmuir* **2004,** 20, (5), 1799-1806.

25. Wang, L. G.; Yoon, R. H., Hydrophobic forces in the foam films stabilized by sodium dodecyl sulfate: Effect of electrolyte. *Langmuir* **2004,** 20, (26), 11457-11464.
26. Wang, J. L.; Yoon, R. H., AFM forces measured between gold surfaces coated with self-assembled monolayers of 1-hexadecanethiol. *Langmuir* **2008,** 24, (15), 7889-7896.
27. Christenson, H. K.; Claesson, P. M., Direct measurements of the force between hydrophobic surfaces in water. *Advances in Colloid and Interface Science* **2001,** 91, (3), 391-436.
28. Yoon, R. H.; Mao, L. Q., Application of extended DLVO theory .4. Derivation of flotation rate equation from first principles. *Journal of Colloid and Interface Science* **1996,** 181, (2), 613-626.
29. Butt, H. J. G. K. K. M., *Physics and Chemistry of Interfaces*. Wiley-VCH: Weinheim, 2003.
30. Adamson, A. W., *Physical Chemistry of Surface. 2nd edition*. Interscience Publishers: New York:, 1967.
31. Derjaguin, B., Disjoining Effect of Free Liquid-Films, and Its Role in the Stability of Foams. *Kolloid Zh* **1953,** 15, 9.
32. Eriksson, J. C.; Toshev, B. V., Disjoining Pressure in Soap Film Thermodynamics. *Colloids and Surfaces* **1982,** 5, (3), 241-264.
33. Allan, R. S.; Charles, G. E.; Mason, S. G., The approach of gas bubbles to a gas/liquid interface. *Journal of Colloid Science* **1961,** 16, (2), 150-165.
34. Platikanov, D., Experimental Investigation on the Dimpling& of Thin Liquid Films. *The Journal of Physical Chemistry* **1964,** 68, (12), 3619-3624.
35. Frankel, S. P.; Myseis, K. J., On the "dimpling" during the approach of two interfaces. *The Journal of Physical Chemistry* **1962,** 66, (1), 190-191.
36. Zorin, Z.; Platikanov, D.; Kolarov, T., The transition region between aqueous wetting films on quartz and the adjacent meniscus. *Colloids and Surfaces* **1987,** 22, (2), 133-145.
37. Fisher, L. R.; Mitchell, E. E.; Hewitt, D.; Ralston, J.; Wolfe, J., The drainage of a thin aqueous film between a solid surface and an approaching gas bubble. *Colloids and Surfaces* **1991,** 52, 163-174.
38. Jain, R. K.; Ivanov, I. B., Thinning and Rupture of Ring-Shaped Films. *Journal of the Chemical Society-Faraday Transactions Ii* **1980,** 76, 250-266.
39. Sheludko, A., Thin liquid films. *Advances in Colloid and Interface Science* **1967,** 1, (4), 391-464.
40. Hartland, S.; Robinson, J. D., A model for an axisymmetric dimpled draining film. *Journal of Colloid and Interface Science* **1977,** 60, (1), 72-81.
41. Dimitrov, D. S.; Ivanov, I. B., Hydrodynamics of thin liquid films. On the rate of thinning of microscopic films with deformable interfaces. *Journal of Colloid and Interface Science* **1978,** 64, (1), 97-106.
42. C.-Y. Lin, J. C. S., Thinning of a liquid film as a small drop or bubble approaches a solid plane. *Aiche Journal* **1982,** 28, (1), 147-156.
43. Jing-Den Chen, J. C. S., Effects of London-van der Waals forces on the thinning of a dimpled liquid film as a small drop or bubble approaches a horizontal solid plane. *Aiche Journal* **1982,** 28, (6), 955-963.
44. Jing-Den Chen, P.-S. H., J. C. Slattery,, Effects of electrostatic double-layer forces on coalescence. *Aiche Journal* **1988,** 34, (1), 140-143.
45. Hewitt, D.; Fornasiero, D.; Ralston, J.; Fisher, L. R., Aqueous Film Drainage at the Quartz Water Air Interface. *Journal of the Chemical Society-Faraday Transactions* **1993,** 89, (5), 817-822.
46. Fisher, L. R.; Mitchell, E. E.; Hewitt, D.; Ralston, J.; Wolfe, J., The Drainage of a Thin Aqueous Film between a Solid-Surface and an Approaching Gas Bubble. *Colloids and Surfaces* **1991,** 52, (1-2), 163-174.

47. Pugh, R. J.; Yoon, R. H., Hydrophobicity and Rupture of Thin Aqueous Films. *Journal of Colloid and Interface Science* **1994,** 163, (1), 169-176.
48. Pushkarova, R. A.; Horn, R. G., Bubble-solid interactions in water and electrolyte solutions. *Langmuir* **2008,** 24, (16), 8726-8734.
49. Pushkarova, R. A.; Horn, R. G., Surface forces measured between an air bubble and a solid surface in water. *Colloids and Surfaces a-Physicochemical and Engineering Aspects* **2005,** 261, (1-3), 147-152.
50. Fielden, M. L.; Hayes, R. A.; Ralston, J., Surface and Capillary Forces Affecting Air Bubble-Particle Interactions in Aqueous Electrolyte. *Langmuir* **1996,** 12, (15), 3721-3727.
51. Ducker, W. A.; Xu, Z.; Israelachvili, J. N., Measurements of Hydrophobic and DLVO Forces in Bubble-Surface Interactions in Aqueous Solutions. *Langmuir* **1994,** 10, (9), 3279-3289.
52. Tchaliovska, S.; Herder, P.; Pugh, R.; Stenius, P.; Eriksson, J. C., Studies of the Contact Interaction between an Air Bubble and a Mica Surface Submerged in Dodecylammonium Chloride Solution. *Langmuir* **1990,** 6, (10), 1535-1543.
53. Yoon, R. H.; Yordan, J. L., The Critical Rupture Thickness of Thin Water Films on Hydrophobic Surfaces. *Journal of Colloid and Interface Science* **1991,** 146, (2), 565-572.
54. Yoon, R. H.; Aksoy, B. S., Hydrophobic forces in thin water films stabilized by dodecylammonium chloride. *Journal of Colloid and Interface Science* **1999,** 211, (1), 1-10.
55. Yoon, R. H., The role of hydrodynamic and surface forces in bubble-particle interaction. *International Journal of Mineral Processing* **2000,** 58, (1-4), 129-143.
56. Wang, L. G.; Yoon, R. H., Hydrophobic forces in thin aqueous films and their role in film thinning. *Colloids and Surfaces a-Physicochemical and Engineering Aspects* **2005,** 263, (1-3), 267-274.
57. Alexandrova, L.; Pugh, R. J.; Tiberg, F.; Grigorov, L., Confirmation of the heterocoagulation theory of flotation. *Langmuir* **1999,** 15, (22), 7464-7471.
58. K. W. Stockelhuber, H. J. S., A. Wenger,, First Experimental Proof of the Nonexistence of Long-Range Hydrophobic Attraction Forces in Thin Wetting Films. *Chemical Engineering & Technology* **2001,** 24, (6), 624-628.
59. Schulze, H. J.; Stokelhuber, K. W.; Wenger, A., The influence of acting forces on the rupture mechanism of wetting films -- nucleation or capillary waves. *Colloids and Surfaces A: Physicochemical and Engineering Aspects* **2001,** 192, (1-3), 61-72.
60. Mahnke, J.; Schulze, H. J.; Stckelhuber, K. W.; Radoev, B., Rupture of thin wetting films on hydrophobic surfaces. Part II: fatty acid Langmuir-Blodgett layers on glass surfaces. *Colloids and Surfaces A: Physicochemical and Engineering Aspects* **1999,** 157, (1-3), 11-20.
61. Mahnke, J.; Schulze, H. J.; Stckelhuber, K. W.; Radoev, B., Rupture of thin wetting films on hydrophobic surfaces: Part I: methylated glass surfaces. *Colloids and Surfaces A: Physicochemical and Engineering Aspects* **1999,** 157, (1-3), 1-9.
62. Stockelhuber, K. W.; Radoev, B.; Wenger, A.; Schulze, H. J., Rupture of wetting films caused by nanobubbles. *Langmuir* **2004,** 20, (1), 164-168.
63. Slavchov, R.; Radoev, B.; Stockelhuber, K. W., Equilibrium profile and rupture of wetting film on heterogeneous substrates. *Colloids and Surfaces a-Physicochemical and Engineering Aspects* **2005,** 261, (1-3), 135-140.
64. Vinogradova, O. I.; Horn, R. G., Attractive forces between surfaces: What can and cannot be learned from a jump-in study with the surface forces apparatus? *Langmuir* **2001,** 17, (5), 1604-1607.
65. Vinogradova, O. I., Drainage of a Thin Liquid-Film Confined between Hydrophobic Surfaces. *Langmuir* **1995,** 11, (6), 2213-2220.

66. Vinogradova, O. I., Slippage of water over hydrophobic surfaces. *International Journal of Mineral Processing* **1999,** 56, (1-4), 31-60.
67. Vinogradova, O. I., Implications of Hydrophobic Slippage for the Dynamic Measurements of Hydrophobic Forces. *Langmuir* **1998,** 14, (10), 2827-2837.

Chapter 2

Hydrophobic Forces in Wetting Films Between Air Bubbles and Hydrophobized Gold Surfaces

Abstract

The kinetics of thinning for the wetting films of water formed on hydrophobic gold substrates has been studied using the thin film pressure balance (TFBC) technique. The changes in film thickness have been monitored by recording the profiles of the dimpled films as a function of time using a high-speed video camera. It was found that the film thinning kinetics as measured at the barrier rims of a film of water formed on a hydrophilic silica surface can be predicted using the Reynolds lubrication approximation with the non-slip boundary condition. The results obtained using the wetting films of water formed on hydrophobized gold substrates showed that the kinetics increases with increasing hydrophobicity. The kinetics data obtained at different hydrophobicities have been fitted to the Reynolds approximation to determine the hydrophobic force constants (K_{132}) of a power law. It was found that K_{132} increases with increasing contact angle and decreases with electrolyte (NaCl) concentration. It was found also that the K_{132} values can be predicted from the hydrophobic force constants (K_{131}) obtained for the interaction between hydrophobic surfaces and the same (K_{232}) for the foam films using the geometric mean combining rule that is frequently used to predict asymmetric molecular forces from symmetric ones.

2.1 Introduction

Properties of the thin liquid films between particles, bubbles and drops control the behavior of their suspensions and interactions with each other. In flotation, air bubbles collide with particles and create wetting films between them. If the films are unstable, particles break the films, attach themselves to the bubbles, and float. If the films are stable, no flotation would occur. Thus, control of the stability of wetting films is of critical importance in flotation. The key parameter controlling the stability of wetting films is the hydrophobicity of particles. Flotation is a rate process, and its kinetics increases with particle hydrophobicity.[1, 2] Various reagents are used to render selected minerals hydrophobic. For sulfide minerals and precious metals, short-chain alkyl xanthates and thionocarbamates are commonly used as hydrophobizing agents (collectors). For the flotation of non-metallic minerals such as silica and iron oxides, long-chain high HLB surfactants are used for hydrophobization. Air bubbles have been in use for minerals flotation since 1905 when the process was first patented,[3] and yet the basic mechanisms involved in the rupture of wetting films are not well understood.

When an air bubble is pressed against a hydrophilic plate such as mica and quartz in water[4-7], the intervening liquid drains until a stable film is formed. The stability of the wetting film arises from the disjoining (or 'wedging-apart') pressure, which was considered to arise from double-layer force, van der Waals-dispersion force, and structural force.[8] The first two were classical colloidal forces, while the third was attributed to the hydrogen bonding between the solid and water molecules in the film. At film thicknesses above 20 nm, double-layer force dominates, while at thicknesses below approximately 10-15 nm dispersion force also contributes to stabilizing the wetting films.[9, 10] The film thickness decreases with electrolyte concentration and the valence of electrolyte.[11] It has also been reported that the wetting films on quartz rupture when the charge of the substrate was reversed by Al^{3+} ions[12] or by a cationic surfactant[13]. Thus, the wetting films on hydrophilic surfaces behave just like a typical colloidal film, for which the DLVO theory may be useful.

Blake and Kitchener[9] used the bubble-against-plate technique to study the wetting films formed on both hydrophilic and hydrophobic silica plates. The hydrophobic silica was prepared by coating the surface with trichloromethylsilane (TMCS). The thicknesses of the aqueous films formed on both substrates were approximately the same, which was attributed to the observation that the methylation did not significantly change the ζ-potentials of quartz. When the film thickness was reduced by KCl addition, however, the film on the hydrophobic surface ruptured spontaneously at a thickness of 64 nm, which was attributed to the presence of hydrophobic force in the wetting film. Tchaliovska *et al*.[14] studied the wetting films on mica hydrophobized with dodecylammonium hydrochloride (DAH) and suggested that both hydrophobic force and attractive electrostatic force are important in determining the film lifetime and the rates of expansion of the meniscus perimeter. More recently, Mahnke *et al.*[15] modeled the rupture of the wetting films formed on methylated glass plates using a long-range hydrophobic force with a decay length of 13 nm, while Churaev[16] discussed the role of hydrophobic force in the rupture of wetting films.

The first direct measurement of hydrophobic force was reported by Israelachvili and Pashley.[17] The measurements were made using the surface force apparatus (SFA) in cetyltrimethyl-ammonium bromide (CTAB) solutions. Many investigators[18] conducted follow-up experiments using SFA and atomic force microscope (AFM) with surfaces coated with various hydrophobizing agents and reported much longer-ranged and stronger hydrophobic forces than reported by Israelachvili and Pashley. However, the origin of the hydrophobic force is not yet known, and many investigators suggested various possible mechanisms. These include electrostatic interaction between the charged domains of adsorbed surfactants,[19] cavition, [20, 21] nanobubbles,[22, 23] and others.[24-26] Of these, the possibility of nanobubbles causing the long-range attractions has received much attention in recent years. It has been shown, however, that long-range attractions were also observed in degassed solutions,[27, 28] although the attraction becomes stronger in the presence of dissolved gases. Further, recent thermodynamic studies showed that macroscopic hydrophobic interactions entail entropy decrease, contrary to the case of molecular-scale hydrophobic interactions.[29, 30] This finding suggests that the long-range hydrophobic force originates from the structural changes in the water present in the confined spaces between hydrophobic surfaces.

The possibility of nanobubbles playing a role in the rupture of wetting films has been explored by some investigators. Stockelhuber *et al*.[31] suggested that the thin liquid films formed between the nanobubbles nucleating on a hydrophobic surface and the air/water interface of a wetting film act like foam films, in which attractive van der Waals force can cause the rupture by the capillary wave mechanism.[32, 33] According to Laskowski *et al*. [34], there are no attractive forces in wetting films; therefore, its rupture cannot be accounted by the capillary wave mechanism.

Platikanov[35] monitored the kinetics of thinning of the wetting films on hydrophilic glass plates. They found that the films formed dimples initially and produced flat films at equilibrium as predicted by Frankel and Mysels.[36] The dimples disappeared, however, when film radii became small. The author showed that the kinetics measured at 0.1 M KCl can be described by Reynolds lubrication approximation with the non-slip boundary condition for both the solid/water and air/water interfaces. Thus, the author concluded that the dynamic method of using the Reynolds approximation can be used to determine the disjoining pressure if liquid films are flat and plane-parallel. Wang and Yoon[37] also used the Reynolds approximation to determine the contributions from the hydrophobic force to the disjoining pressures in single foam films. They found that air bubbles are hydrophobic and that the hydrophobic force in foam films decreases with increasing surfactant and NaCl concentrations.

Schulze and his co-workers[10] measured the critical rupture thicknesses of the wetting films formed on hydrophobic surfaces and compared the results with the film thinning kinetics predicted using the Reynolds equation. Without recognizing the presence of hydrophobic force, the authors suggested that the kinetics of film thinning should follow the same theoretical curve, because the surface charge did not change after hydrophobization with hexamethyldisilazane (HMDS). It was found that the critical rupture thicknesses plotted *vs*. film lifetime were randomly distributed around the theoretical thinning curve, which lead to their conclusion that films rupture due to the presence of gas nuclei formed on heterogeneous surfaces and the hole formation

mechanism suggested by Sharma and Ruckenstein.[38] More recent work of Sharma[39] suggested, however, that the hole formation is due to hydrophobic attraction.

In the present work, we monitored the kinetics of thinning of wetting films using the TFPB technique. Water films were formed on gold plates hydrophobized with potassium amyl xanthate (PAX). The kinetics was monitored by means of a high-speed video camera, which allowed accurate measurements of film thicknesses changing with time at any point of a dimpled film. The results were analyzed using the Reynolds approximation with the non-slip boundary condition to determine the disjoining pressures. It was found that the kinetics of film thinning increases with increasing hydrophobicity, which was attributed to the increase in hydrophobic force in wetting films. The magnitudes of the hydrophobic forces measured in the wetting films were compared with those measured in foam films and in the films between hydrophobic solid surfaces.

2.2 Theoretical Approach

When an air bubble is pressed against a flat solid surface in a horizontal orientation, the air/water interface deforms to produce initially a plane-parallel wetting film. The change in curvature associated with the deformation creates a pressure difference between the liquid in the film and the bulk and causes the film to thin. As the thinning continues, the film becomes a convex lens (or "dimple") with inverted curvature. The torus-shaped water film surrounding a dimple is referred to "barrier rim". The dimpled film is no longer plane parallel, but many investigators[40, 41] modeled the thinning process using the Reynolds lubrication approximation, which has been derived using the boundary conditions that the two interfaces are parallel to each other and that the liquid velocity at the two interfaces are zero, *i.e.*, the film thins under no slip conditions. The radii of the barrier rings observed in the present work were larger than 0.08 mm, while we were monitoring the thinning rate at film thicknesses below approximately 300 nm. The large difference in the length scales should satisfy the first boundary condition. Maali *et al.*[42] showed that the non-slip boundary condition is appropriate for the water flow on the hydrophilic surface. Also, Lin and Slattery[43] showed that the air/water interfaces are immobile in the presence of a trace of surfactant. Platikanov[35] and Frankel *et al.*[36] showed that the Reynolds lubrication approximation can be used to model the thinning of wetting films at the barrier ring.

The Reynolds lubrication approximation is usually presented in the following form:[44]

$$\frac{dh}{dt} = -\frac{2h^3\Delta P}{3\mu R_f^2} \qquad [1]$$

where h is film thickness, t drainage time, μ the liquid viscosity, R_f the film radius, and ΔP is the pressure difference causing a film to thin. In dimpled wetting films, the ΔP may be expressed as follows,[45]

$$\Delta P = \frac{2\sigma}{R} - \Pi - \frac{\gamma}{r}\frac{\partial}{\partial r}\left(r\frac{\partial h}{\partial r}\right) \qquad [2]$$

where R is the radius of film holder (or bubble), γ the surface tension of liquid, r the radial distance from the center of the barrier ring, h the local film thickness, and Π is the disjoining pressure. The first term represents the contribution from the Laplace pressure, the second term from the hydrodynamic pressure due to changes in curvature along the radial distance, and the third tem represents the contribution from the disjoining pressure created by the surface forces in the film.

Thus, wetting films thin by hydrodynamic forces initially and then by surface forces during the later stages. In thin films, the contribution from the changes in curvature ($\partial h / \partial r$) may not be important as the curvature around a barrier rim becomes symmetrical, as will be shown later (Figure 2). In this case, Eq. [2] is reduced to:

$$\Delta P = \frac{2\gamma}{R} - \Pi \qquad [3]$$

The DLVO theory recognizes two surfaces forces, *i.e.*, double-layer force and van der Waals dispersion force. The latter is repulsive in wetting films,[34] while the former can also be repulsive in alkaline pH where both the solid/water and air/water interfaces are usually charged negatively. Despite the absence of an attractive force, wetting films formed on hydrophobic surfaces rupture. We, therefore, use the extended DLVO theory,[1]

$$\Pi_t = \Pi_d + \Pi_e + \Pi_h \qquad [4]$$

which includes disjoining pressures due to the van der Waals-dispersion force (Π_d), double-layer force (Π_e), and hydrophobic force (Π_h).

The disjoining pressure due to the van der waals force can be given by,

$$\Pi_d = -\frac{A_{132}}{6\pi h^3} \qquad [5]$$

where A_{132} is the Hamaker constant for the interaction between a solid **1** and an air bubble **2** in water **3**. A_{132} can be obtained using the geometric mean combining rule from the values of the Hamaker constants for the interactions between solids in water (A_{131}) and between bubbles in water (A_{232}). In the present system, dispersion forces are much smaller than hydrophobic forces; therefore, the retardation effect has not been considered.

The electrostatic component of the disjoining pressure can be calculated using the Hogg-Healey-Fuerstenau (HHF) approximation,[46]

$$\Pi_e = -\frac{\varepsilon\kappa^2}{2\sinh(\kappa h)}\left[(\Psi_1^2 + \Psi_2^2)\operatorname{cosech}(\kappa h) - 2\Psi_1\Psi_2\coth(\kappa h)\right] \qquad [6]$$

in which ε is the dielectric permittivity of water, Ψ_1 and Ψ_2 are the double-layer potentials at the solid/water and air/water interfaces, respectively, and κ is the inverse Debye length.

Hydrophobic forces measured in experiments are usually represented in single- or double-exponential functions. It has been shown that a power law of the following form can also be used,[47, 48]

$$\Pi_h = -\frac{K_{132}}{6\pi h^3} \quad [7]$$

where K_{132} is a constant representing the magnitude of the hydrophobic force in a wetting film of thickness h. Eq. [7] is of the same form as Eq. [5], which makes it easier to compare K_{132} directly with A_{132}.

2.3 Experimental Details

Materials

Polished fused quartz plates (Technical Glass Inc.) and gold-coated glass plates (CA134, EMF) were used as substrates for wetting films. Potassium amyl xanthate (PAX, >90%, TCI, America) was purified twice by dissolution in acetone (HPLC, Fisher Sci.) and recrystallization in diethyl ether (99.999%, Sigma-Alrich). Sodium chloride (99.999%, Sigma-Aldrich) was roasted at 600°C for 6 hours to remove organic impurities. All solutions were prepared using the Millipore water of >18.2 MΩ/cm, which was obtained using a Direct-Q3 water purification system.

Procedure

Both the fused quartz and gold plates were cleaned by boiling in piranha solutions (7:3 by volume of H_2SO_4:H_2O_2) for 30 minutes, followed by rinsing with the Millipore water and drying in a nitrogen gas stream. After the cleaning, the gold plates were hydrophobized by immersing them in freshly prepared PAX solutions. The hydrophobicity was controlled by varying the concentration and immersion time. The treated surfaces were washed with Millipore water and dried by blowing high-purity nitrogen gas on the surface. The quartz was used as substrate for wetting films without hydrophobization.

The kinetics of film thinning was measured using the TFPB technique, which was originally designed to study foam films.[32] A flat substrate was placed on top of a film holder (2.0 mm radius) immersed in water. After making sure that no air bubbles were adhering on the surface, the assembly was placed on an inverted microscopic stage (Olympus IX51) to monitor the changes in film thickness with time. A halogen lamp (100W, Osram) was used as a light source with a band-pass filter (NT46-053, Edmund Optics) to produce monochromatic green light source (λ=526 nm).

Initially, the thickness of a film was reduced by pulling the water out of the film holder by means of a piston. Once interference patterns (Newton rings) began to appear in the microscopic field of view, the film was allowed to thin spontaneously while recording the images by means of a high-speed CCD camera (Fastcam 512PCI, Photron) at a speed of 60 frames per second. The

camera was capable of taking the images at much higher speeds, but 50 FPS was found to be adequate. The interference patterns recorded were used to obtain timed profiles of a wetting film across the entire film holder, which in turn were used to monitor the changes in film thicknesses (h) as a function of time at any point of the film. The film thicknesses were calculated as described by Nedyalkov *et al*.[49]

The surface tensions of the solutions used in the present work were measured using the Wilhelmy plate method. Advancing and receding contact angles of the hydrophobized gold plates were measured using the sessile drop technique by means of a goniometer (Ramé-Hart, Inc.).

The ξ-potentials of spherical gold power (1.5-3.0 μm, Alfa Aesar) were measured by dynamic light scattering (Zetasizer Nano). The gold power (99.96%) was hydrophobized in the same manner as the gold plate used for the film thinning kinetics measurements. It was assumed that the ξ-potentials of the gold plate and powder were the same.

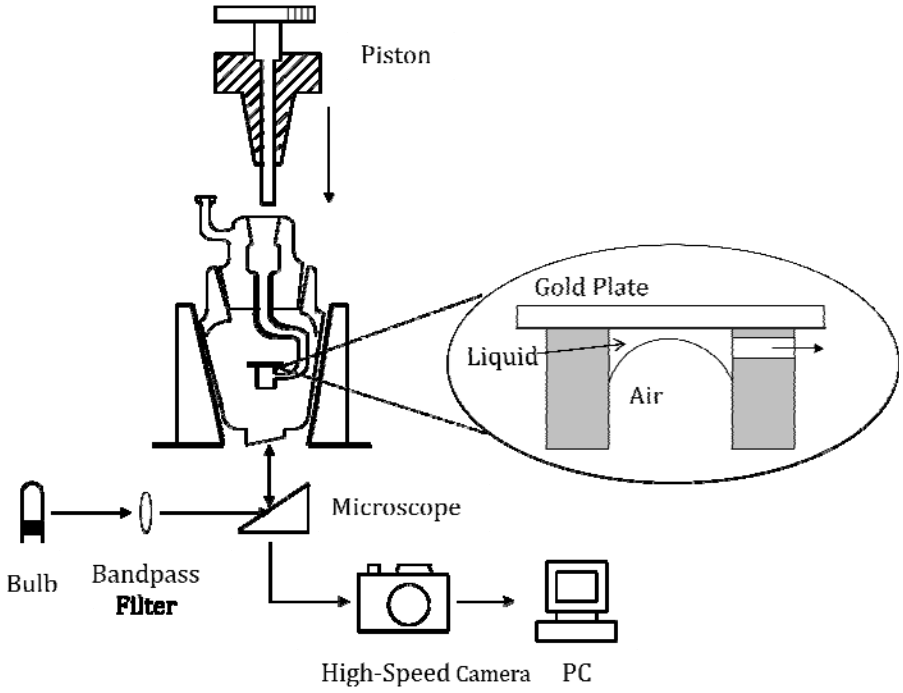

Figure 1. Schematics of the TFBC apparatus used for the study of wetting films

2.4 Results

Figure 2 compares the timed profiles of the wetting films formed on gold substrates of two different hydrophobicities. Figure 2a shows the profiles of the film formed on a freshly-cleaned

gold plate that had not been hydrophobized. Its equilibrium contact angle (θ_e) was 42° with 60° advancing (θ_a) and 17° receding (θ_r) angles. Initially, the film showed dimpled profiles. As the drainage continued, the film became flat and reached an equilibrium thickness (h_e) of 80 nm in 20 s, when the capillary pressure was equal to the disjoining pressure. Figure 2b shows the timed profiles of the wetting film formed on a gold plate hydrophobized in a $5x10^{-6}$ M PAX solution for 60 min to obtain $\theta_r = 79°$. The drainage rate became substantially faster than observed with the untreated gold plate; the film thickness decreased from 300 to 80 nm in 1.26 s and ruptured. The thickness at which the film fails catastrophically is referred to as critical rupture thickness (h_{cr}). Note that the dimpling effect was more significant with the hydrophobic gold, indicating that the wetting film formed on the hydrophobic surface thins faster at the barrier rim than at the center. Note also that the curvature of the air/water interface on either side of the barrier rim was about the same, which would allow one to ignore the hydrodynamic pressure term of Eq. [2] during the last stages of the film thing process.

Fig. 3 shows the changes in thickness of a wetting film formed on a hydrophilic fused quartz plate at its center and at the barrier rim. The measurements were conducted in a 0.1 M NaCl solution so that the Π_e term of Eq. [4] can be ignored. Since the substrate was hydrophilic, Π_h was also ignored. Eq. [3] can then be reduced to,

$$\Delta P = \frac{2\gamma}{R} - \Pi_d = \frac{2\gamma}{R} - \frac{A_{132}}{6\pi h^3} \qquad [8]$$

By using the values of γ = 72.4 mN/m at 0.1 M NaCl and $A_{132} = -1.13x10^{-20}$ J,[50] the kinetics curve obtained at the barrier rim was fitted to Eq. [1]. The fit was excellent indicating that one can safely use the Reynolds approximation to describe the kinetics of wetting films. The results showed that the non-slip condition applies to both the surfactant-free quartz-water interface and the free air-water interface. The kinetics curve obtained at the center of the dimple thins slower than at the rim. The results presented in Figure 3 are similar to the work of Platikanov. [35]

Figure 4 compares the kinetics of film thinning on gold substrates with and without hydrophobization. After one hour of immersion time in a $5x10^{-6}$ M PAX at open circuit and natural pH (= 7.3), the gold plate was rendered hydrophobic with θ_r = 79°. The untreated gold plate showed only a slight hydrophobicity with θ_r = 17° possibly due to contaminants. When a gold surface was freshly cleaned in a piranha solution, the contact angle was zero. But the angle increased considerably after a short exposure to the atmosphere, during which time contaminants could adsorb on the surface from the air owing to the large Hamaker constant of gold. Despite the apparent but a low-level hydrophobicity, its kinetics was much slower than on the treated surface, as shown in Figure 4, and the film did not rupture. On the contrary, the wetting film on formed on the treated gold surface ruptured at h_{cr} = 80 nm and thinned substantially faster, which may be attributed to the presence of hydrophobic force in the wetting film.

In general, xanthate-coated mineral surfaces are negatively charged in water, and the ζ-potentials do not change substantially at low concentrations.[51] Also, xanthate adsorption should not change the Hamaker constant of the gold plate (A_{131}) significantly. For the experiment conducted with the hydrophobic gold, the substrate was hydrophobized prior to forming a wetting film with pure water. Therefore, the chemistry of the air/water interface should be the same as

that of the experiment conducted with untreated gold, that is, the ζ-potential and the Hamaker constant of the air bubble (A_{232}) should essentially be the same as those of the untreated gold surface. It is, therefore, suggested that the fast kinetics of the film thinning on the hydrophobic surface was due to the hydrophobic force. We estimated the magnitude of the hydrophobic force by fitting the kinetics curves to the Reynolds equation (Eq. [1]). ΔP was calculated using Eqs. [3]-[7]. The values of the various parameters used for the fit are given in Figure 4. In calculating the contribution from the hydrophobic force (Π_h), it was necessary to use the values of K_{132} = $2.0\text{x}10^{-17}$ J for the hydrophobized gold substrate and $K_{132} = 0$ for the untreated substrate. Note here that K_{132} was positive and that its magnitude was much larger than that of the Hamaker constant (A_{132} = $-2.02\text{x}10^{-20}$ J), which was negative.

Figure 5 shows the results of the kinetics studies conducted with gold-coated silica plates by varying the immersion time in a 10^{-5} M PAX solution. The film thicknesses were measured at the barrier rims of the timed film profiles. It was found that the film thinning kinetics was the fastest after 10 minutes of immersion time and became slower at longer contact times. The results obtained after the 10-min contact time was fitted to the Reynolds equation with $K_{132} = 2.0\text{x}10^{-17}$ J. After a 120 min immersion time, K_{132} decreased to $7.0\text{x}10^{-18}$ J and the drainage rate decreased, which may be attributed to a multilayer formation. It is well known that xanthate adsorption on sulfide minerals and precious metals results in the formation of a multilayer.[52-54] Xanthate adsorption results in the formation of chemisorbed xanthates in the first monolayer, followed by the adsorption of metal xanthates and/or dixanthogen on the top at higher electrochemical potentials.[55, 56] Evidences for the multilayer formation in the gold-PAX system after long contact times and higher concentrations have been presented in another communication.[57] Note that θ_r was 78° after 10 min contact time, which decreased to 75° after the 120 min contact time. Albeit small, the decrease in contact angle may be a reflection of the fact that the species adsorbing in the multilayer expose the head groups (-OCSSAu) toward the aqueous phase. Although the head group should be less hydrophobic than the end group (CH_3) of the chemisorbed xanthate in the monolayer, it may be substantially less polar than those of the high HLB number surfactants, providing an explanation for the relatively small decrease in θ_r observed in the present work. The decrease in K_{132} with increasing contact time may thus be attributed to the decrease in the hydrophobicity of the gold substrate. This finding is consistent with the results of the AFM force measurements conducted between xanthate-coated gold sphere and gold plate.[57] It is also possible that the multilayer formation increases the roughness of the xanthate-coated gold plate, which should also contribute to the decrease in the drainage rate and hence the K_{132} values estimated using the Reynolds approximation.

After the 10 min contact time, which was considered short enough to prevent the multilayer formation, a set of timed film profiles have been obtained at different PAX concentrations (10^{-6} to 10^{-4} M), and the changes in film thickness at the barrier rims have been monitored and plotted in Figure 6. The receding contact angle (θ_r) increased from 65° at 10^{-6} M to 80° at 10^{-5} M PAX. As expected, drainage rate increased with increasing PAX concentration and θ_r, suggesting that the increased kinetics was due to the increased hydrophobic force in the wetting films. Figure 7 shows the K_{132} values obtained by fitting the kinetics data to Eq. [1] plotted *vs*. the PAX concentration. As shown, K_{132} increased with increasing concentration and reached a maximum at approximately $3\text{x}10^{-5}$ M. The data presented in Figures 6 and 7 provides strong evidence that

hydrophobic force exists in the wetting films formed on hydrophobic surfaces and serves as the major driving force for the film drainage and rupture.

Figure 8 shows the effect of electrolyte (NaCl) on the kinetics of film thinning on hydrophobic surfaces. The experiments were conducted with gold plates treated in $5x10^{-6}$ M PAX solutions for 60 minutes. Also shown for comparison is the result (dashed line) obtained with a wetting film formed with pure water on the surface of an untreated gold plate. In the absence of NaCl, the wetting film formed on hydrophobized gold plate thinned substantially faster than that formed on untreated hydrophilic plate, which can be attributed to the presence of a strong hydrophobic force in the former. The kinetics curve obtained with the hydrophobic gold in the absence of NaCl can be fitted to the Reynolds equation with $K_{132} = 2.0x10^{-17}$ J. In the presence of 10^{-5} M NaCl, K_{132} decreased to $1.6x10^{-17}$ J, causing a decrease in the kinetics of film thinning. At 10^{-4} and 10^{-3} M NaCl, K_{132} decreased further to $6.0x10^{-18}$ and $5.5x10^{-18}$ J, respectively, with a further decrease in the kinetics. Table 1 shows the various parameters used to fit the data presented in Figure 8 to the Reynolds equation.

That the hydrophobic force in wetting films decreased in the presence of NaCl was consistent with the results from the AFM[58, 59] and foam film[60, 61] studies that the hydrophobic forces in the thin films confined between solid surfaces and between air bubbles decrease in the presence of electrolytes. It was suggested that electrolytes can break the hydrogen bonds between water molecules and, hence, cause a decrease in cohesive energy (W_c) and hydrophobic force.[60] The observation that the drainage rate of the wetting films formed on the hydrophobic surfaces decreased in the presence of NaCl appeared to be contrary to the DLVO theory, according to which the kinetics should actually increase due to double-layer compression. This apparent discrepancy simply indicates that the decrease in the attractive hydrophobic force was greater than the decrease in the repulsive electrostatic force due to double layer compression.

2.5 Discussion

We have shown that the wetting films formed on horizontal, planar surfaces begin to thin due to the capillary forces created by the changes in curvature. Its drainage rate can be predicted by the Reynolds lubrication approximation, with the capillary pressure serving as the driving force. As the film continues to thin, the solid/water and air/water interfaces interact with each other and create a disjoining pressure (Π), which also begins to affect the kinetics of film thinning.

Apart from the kinetics of film thinning, whether a film ruptures or not is determined by thermodynamics. When a wetting film ruptures, a new interface, *i.e.*, solid-gas interface, is created at the expense of solid-liquid and solid-gas interfaces. Thus, the Gibbs free energy change (ΔG) associated with the rupture can be given by the following relation:

$$\Delta G = \gamma_{12} - \gamma_{13} - \gamma_{23} < 0 \qquad [9]$$

where γ_{12}, γ_{13}, and γ_{23} represent the free energies at the interfaces between solid **1**, air **2,** and water **3** phases. Combining Eq. [9] with the Young's equation

$$cos\theta = \frac{\gamma_{12} - \gamma_{13}}{\gamma_{23}} \quad [10]$$

where θ is water contact angle, one can find that wetting films rupture when

$$\Delta G = \gamma_{12}(cos\theta - 1) < 0 \quad [11]$$

Eq. [11] suggests that wetting films can rupture when $\theta > 0$ at a critical rupture thickness (h_{cr}). Receding angles (θ_r) may be relevant for the rupture of wetting films. If $\theta = 0$, a wetting film should stabilize at an equilibrium thickness (h_e). We have shown in the present work that the wetting films formed on gold substrates rupture when the surface is rendered hydrophobic by PAX.

From Eqs. [10] and [11], one can see that $\Delta G < 0$ when

$$\gamma_{12} - \gamma_{13} < \gamma_{23} \quad [12]$$

One can substitute the following relation into Eq. [12],[64]

$$\gamma_{13} = \gamma_{12} + \gamma_{23} - 2\sqrt{\gamma_1^d \gamma_3^d} - 2\sqrt{\gamma_1^+ \gamma_3^-} - 2\sqrt{\gamma_1^- \gamma_3^+} \quad [13]$$

where γ_1^d is the dispersion component of solid surface tension, γ_2^d is the same of liquid surface tension, γ_1^+ and γ_1^- are the acidic and basic components of the solid surface tension, respectively, γ_3^+ and γ_3^- are the acidic and basic components of the liquid surface tension, respectively, to obtain:

$$\left(2\sqrt{\gamma_1^d \gamma_3^d} - 2\sqrt{\gamma_1^+ \gamma_3^-} - 2\sqrt{\gamma_1^- \gamma_3^+}\right) < 2\gamma_{13} \quad [14]$$

Eq. [14] is equivalent to the following:

$$W_{ad} < W_c \quad [15]$$

where W_{ad} is the work of adhesion of water on a solid and W_c is the work of cohesion of water. In general, the dispersion component of W_{ad}, *i.e.*, $2\sqrt{\gamma_1^d \gamma_3^d}$, is smaller than W_c. It is, therefore, necessary to decrease the acid-base components of W_c, *i.e.* $2\sqrt{\gamma_1^+ \gamma_3^-}$, and $2\sqrt{\gamma_1^- \gamma_3^+}$, by appropriate surface treatment such as PAX adsorption on gold.

Eqs. [9] and [15] show that spreading coefficient (S) becomes negative when $\theta > 0$, that is, a liquid film retreats and creates a finite solid/liquid interfacial area of contact. The larger the contact angle, the larger the area of contact between bubble and particle, and thereby help minimize the probability of detachment of particles during flotation. (One should note here that advancing contact angles are relevant in detachment.) If a particle makes a point-to-point contact, it will be difficult to levitate coarse particles during flotation. On the other hand, ultrafine particles can be floated without film rupture, *i.e.*, when $\theta = 0$. In dissolved air flotation (DAF), which is widely used for waste water treatment, fine particles are often floated without using

hydrophobizing agents. Control of surface forces, *e.g*., double-layer forces by control of pH and coagulant addition, is sufficient.

Even if film rupture is thermodynamically favorable, the process can be kinetically hindered, *e.g*., by increasing Π, creating surface roughness to slow down drainage rate, increasing film elasticity, *etc*. We have considered that Π consists of dispersion (Π_d), electrostatic (Π_e), and hydrophobic (Π_h) components, as shown in Eq. [4]. Π_d is repulsive as A_{132} is negative in wetting films, while Π_e is also negative in the gold-xanthate system studied here and in many other systems. We found that the kinetics of film thinning increases with increasing xanthate concentration and contact angle (θ_r), which suggests that hydrophobic force is present in the wetting films formed on hydrophobic surfaces. Using the Reynolds lubrication approximation, we calculated the values of K_{132} representing the magnitudes of Π_h (and of hydrophobic forces), which have been found to increase with θ_r. We found also that by recognizing the presence of hydrophobic force in wetting films, it was not necessary to invoke the capillary wave models.[32, 33] The wetting films ruptured spontaneously at h_{cr}. In the gold-PAX system, Π_h was the only negative component of Π and hence could bring the film thickness to h_{cr} in a short time frame. Likewise, Manica *et al*.[45] found that when Π_e is strongly negative, there was no need to invoke the capillary wave model to predict the thinning and rupture of the water films between mica and mercury.

That hydrophobic force is present in wetting films may be more readily acceptable if one can recognize that air bubbles in water are hydrophobic. In this case, the thinning and rupture of the wetting films formed on hydrophobic surfaces may be viewed as one of asymmetric hydrophobic interaction. van Oss *et al*.[64] suggested that the air side of the air-water interface is the most hydrophobic surface known and is about 30% more hydrophobic than octane and Teflon. The basis of this argument is that the tension at the air/water interface (72 mN/m) is substantially higher than those (~50 mN/m) at the hydrocarbon/water interfaces. The vibrational sum frequency (VSF) spectra of the water molecules straddling at the hydrophobic surface/water interfaces show sharp peaks at 3600-3700 cm^{-1}, which represent the characteristic non-hydrogen-bonded (free) OH stretch vibrations.[65, 66] The high interfacial tensions at the hydrophobic surface/water interfaces are due to the presence of the free OH groups at these interfaces. Interestingly, the free OH peaks observed at the CCl_4/water and hexane/water interfaces are observed at 3669±1 cm^{-1}, while the same is observed at ~3700 cm^{-1}. The red shift of the characteristic peak shows an attractive interaction between the free OH groups and the organic molecules at the interface. In fact, the binding energy for the CCl_4-H_2O dimer has been reported to be -1.4 kcal/mol.[66] These reports are consistent with the fact that the dispersion components of W_a at the hydrophobic liquid/water interfaces are ~20 mJ/m^2, while it should be zero at the air/water interface.

We used the Reynolds lubrication approximation to estimate the K_{132} values for hydrophobic disjoining pressure (Eq. [7]). There are several questions to be raised in this approach. First, the approximation is useful for a film of fluid between nearly plane-parallel surfaces. Although we monitored the rate of film thinning at the barrier rim, which is a curved surface, the film thickness (h) was much smaller than the radius of curvature. Therefore, we have measured the thinning rates effectively between plane-parallel surfaces. Second, the roughness of the surface should

affect drainage rate and, hence, the K_{132} values obtained using the Reynolds approximation. In the present work, we found that drainage rate decreased with increasing contact time in PAX solutions due to decreased hydrophobicity and the surface roughness created by multilayer formation.

Perhaps the most important question to be raised would be the question regarding the non-slip boundary condition employed in deriving the Reynolds approximation. There seems to be no doubt that it applies for the flows around hydrophilic surfaces.[42] For the flows around hydrophobic surfaces, however, some found that the non-slip condition may not be applicable. On the other hand, the correlation between slip lengths and contact angle was very poor.[67] As for the flow around air bubbles (or air/water interface), it was found that the liquid/gas interface becomes nearly immobile even with only a trace of surfactant present.[68] Although we have conducted experiments in the absence of surfactants, there is a possibility that trace of gold xanthates be present at the air/water interface, making it possible to use the non-slip condition. If not, the K_{132} values determined in the present work may have been overestimated and require appropriate corrections in future work. Nevertheless, it is highly unlikely that the correction would relinquish the possibility that hydrophobic force is present in the wetting films formed on hydrophobic surfaces. It should be noted also that Horn and his co-workers found that the non-slip boundary condition applies for the surfactant-free mica-water-mercury systems.[45] Further, the drainage experiments conducted in the present work (see Figure 3) and by Platikanov[35] with wetting films produced with surfactant-free air/water interface could be fitted to the Reynolds approximation with non-slip boundary conditions.

The geometric mean combining rule is used to predict the Hamaker constants for van der Waals interactions between unlike surfaces from those between like ones. It is based on the Berthelot relation derived originally for molecular interactions.[69] It has been reported previously that asymmetric hydrophobic force constants (K_{132}) can be predicted using the geometric mean combining rule as follows:[48]

$$K_{132} = \sqrt{K_{131}K_{232}} \qquad [16]$$

in which K_{132} is the force constant for symmetric hydrophobic interaction between two surfaces of identical contact angle of θ_1, and K_{232} is the same for contact angle θ_2.

In Figure 9, the values of K_{132} obtained using the Reynolds approximation have been plotted *vs*. the values of K_{131} in logarithmic scales. According to Eq. [16], the slope should be ½. From the intercept obtained numerically, we found that $K_{232} = 5.3\text{x}10^{-17}$ J. This value is close to that estimated by extrapolating the K_{232} values for the foam films stabilized at different concentrations of ionic and non-ionic surfactants.[60] The K_{131} values used in the plot shown in Figure 9 include those by Wang and Yoon[57] and those measured specifically for the present work using the AFM force measurements conducted with PAX-coated gold surfaces in pure water. It is interesting that Eq. [16] applies for the hydrophobic interactions between solid/liquid, gas/gas, and gas-solid interactions. This finding suggests that hydrophobic force may be a molecular force representing the properties of the thin liquid films confined between hydrophobic surfaces, regardless of whether the interacting surfaces are solid, liquid, or gas. This finding is consistent with the results

of the thermodynamic studies conducted by one of us showing that hydrophobic force may originate from the changes in water structure as a thick film becomes a thin film.[70]

2.6 Summary

The results of present investigation show that the kinetics of thinning for the wetting films of water formed on hydrophilic silica surface can be fitted to the Reynolds lubrication approximation with non-slip boundary conditions. The same approach has also been used to study the kinetics of film thinning on the surface of gold substrates hydrophobized by KAX. The results show that the kinetics increases with increasing hydrophobicity. This finding suggests that hydrophobization of a substrate causes the disjoining pressure in the wetting films to decrease, which in turn can be attributed to the presence of hydrophobic force in the wetting films. It has been found that the hydrophobic force constant (K_{132}) of the wetting film, as determined by fitting the kinetics data to the Reynolds approximation, increases with increasing receding contact angle of the substrate. It has been found also that K_{132} decreases with increasing NaCl concentration and after an excessively long contact time between the substrate and KAX. The former can be attributed to the decrease in the cohesive of energy of water (W_c) in the presence of the electrolyte, while the latter to the increase in surface roughness associate with a possible multilayer formation. Further, the values of K_{132} can be predicted from the values of the hydrophobic force constants (K_{131}) for the interaction between solid surfaces of identical hydrophobicity and those (K_{232}) for the soap films using the geometric mean combining rule.

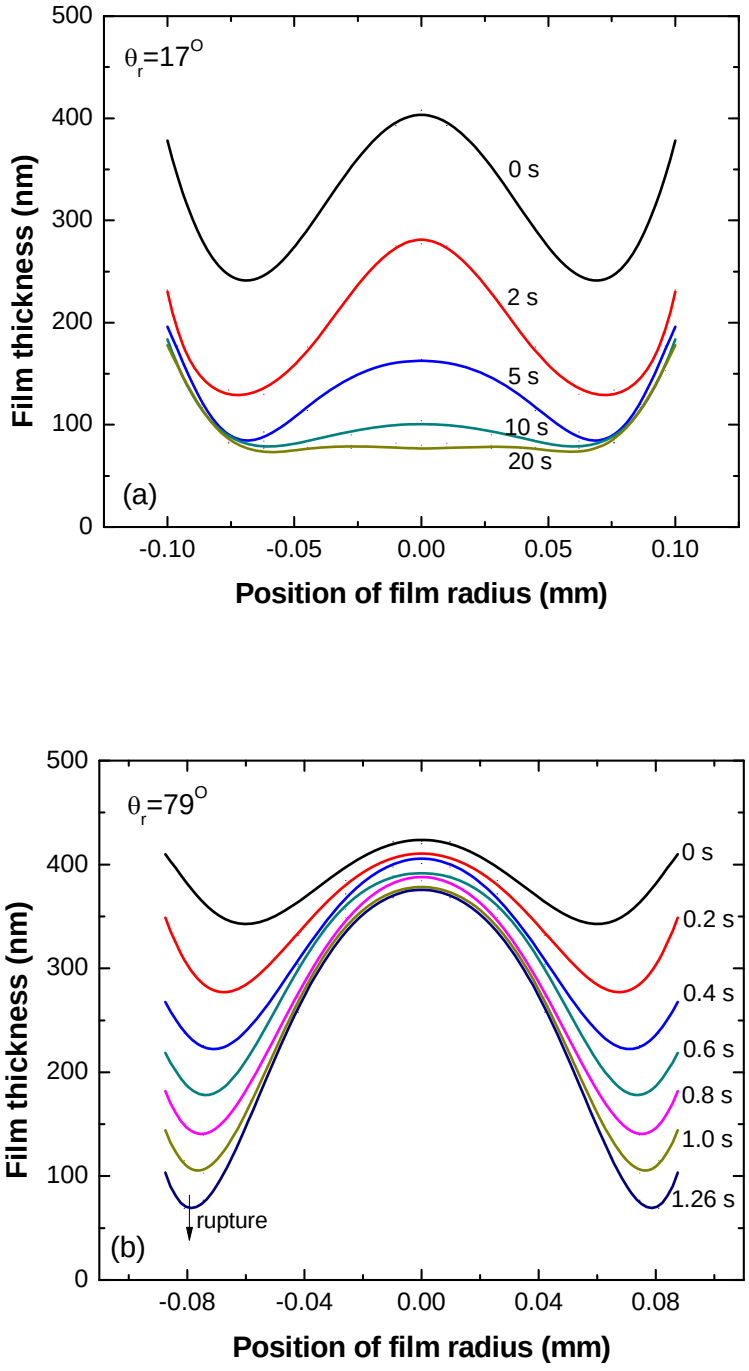

Figure 2.1 Comparison of the timed-profiles of the wetting films formed on a) an untreated gold plate with $\theta_r = 17^o$ and b) a gold plate with $\theta_r = 79^o$ after treatment with a $5x10^{-6}$ M PAX solution for 1 hour.

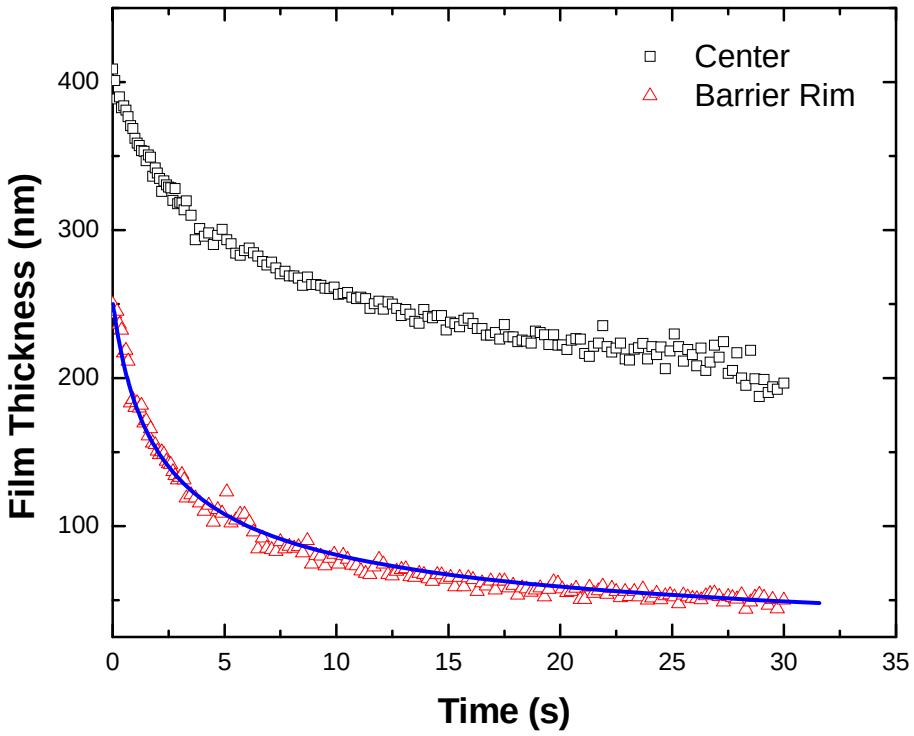

Figure 2.2 Changes in the thickness of a wetting film formed on a hydrophilic fused silica plate in a 10^{-1} M NaCl solution. The solid line represents a fit to Eq. [1] with R_f = 0.084 mm, A_{132} = -1.13x10^{-20} J, and γ = 72 mN/m.

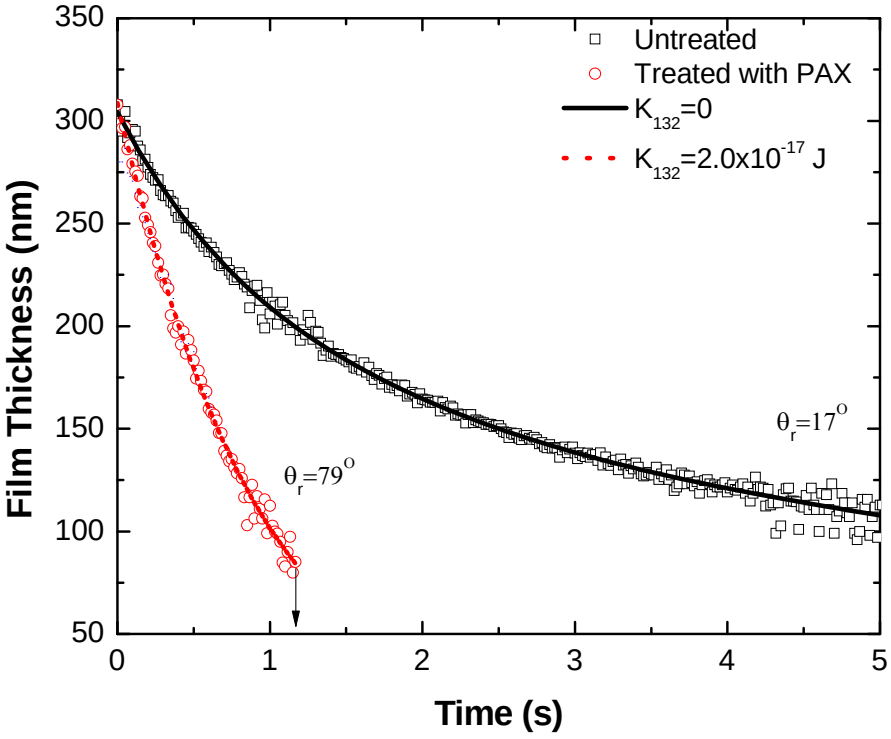

Figure 2.3 Changes in the film thicknesses measured at the barrier rims of the dimpled-wetting films formed on gold-coated silica plates with θ_r of 17° and 79°. The latter was immersed in a 5x10-6 M PAX solution for one hour, and the former was untreated. The solid line represents the Reynolds approximation with $K_{132} = 0$, while the dashed line represents the same with $K_{132} = 2.0 \times 10^{-17}$ J, R_f = 0.075 mm, γ = 72.5 mN/m, Ψ_1 = -45 mV, Ψ_2 = -80 mV, κ^{-1} = 243 nm, and $A_{132} = -2.02 \times 10^{-20}$ J.

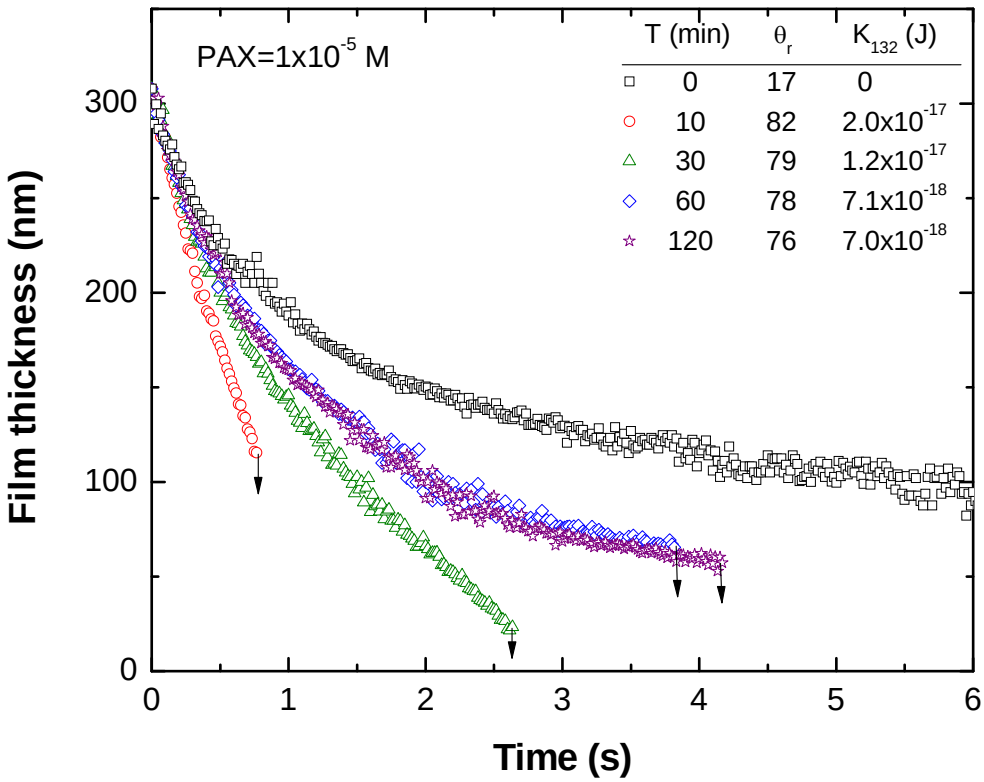

Figure 2.4 Effect of contact time between gold in a 10^{-5} M PAX solution on the kinetics of film thinning. The K_{132} values were by fitting the data to Eq. [1] with γ = 72.5 mN/m, Ψ_1 = -45 mV, Ψ_2 = -80 mV, κ^{-1} = 243 nm, A_{132} = -2.0x10^{-20} J, and R_f = 0.075 $\pm$ 0.004 mm.

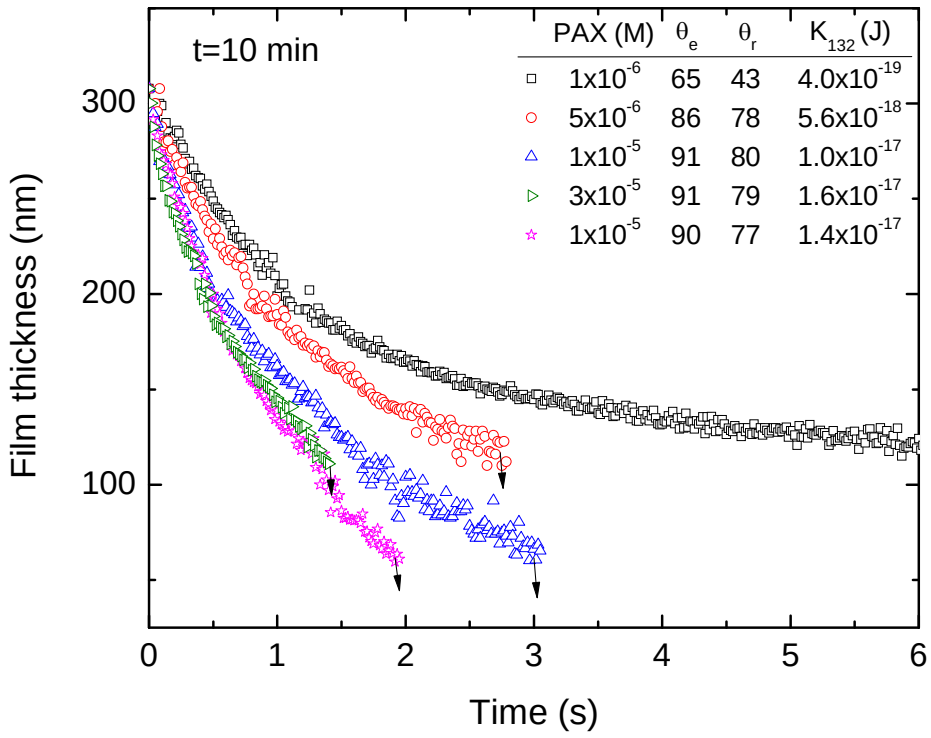

Figure 2.5 Effect of KAX concentration on the thinning of the wetting films formed on gold substrates. The contact time was 10 minutes, and the results were used obtain the K_{132} values using Eq. [1], with γ = 72.5 mN/m, Ψ_1 = -45 mV, Ψ_2 = -80 mV, κ^{-1} = 243 nm, A_{132} = -2.02x10^{-20} J and R_f = 0.091, 0.087, 0.084, 0.08 and 0.076 mm respectively.

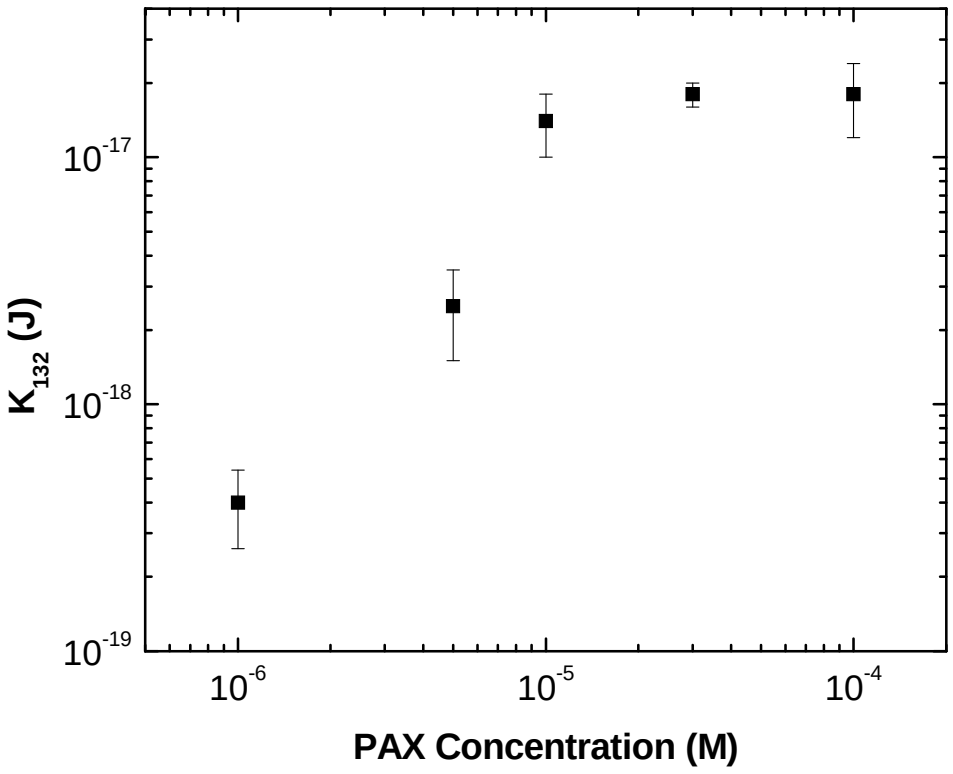

Figure 2.6 Changes in the hydrophobic force constant (K_{132}) with the concentration of KAX solutions, in which gold substrates were hydrophobized for 10 minutes.

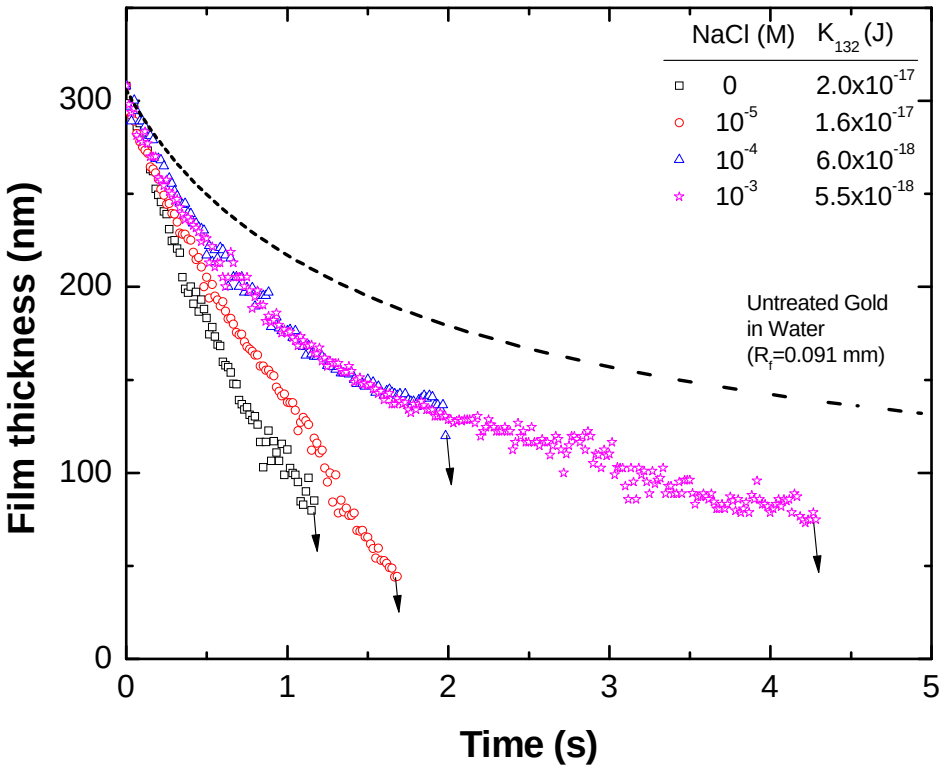

Figure 2.7 Effect of electrolyte (NaCl) on the kinetics of the wetting films formed on the surface of gold-coated glass plates hydrophobized in a $5x10^{-6}$ M PAX solution for 60minutes. The dashed curve represents the results obtained in pure water.

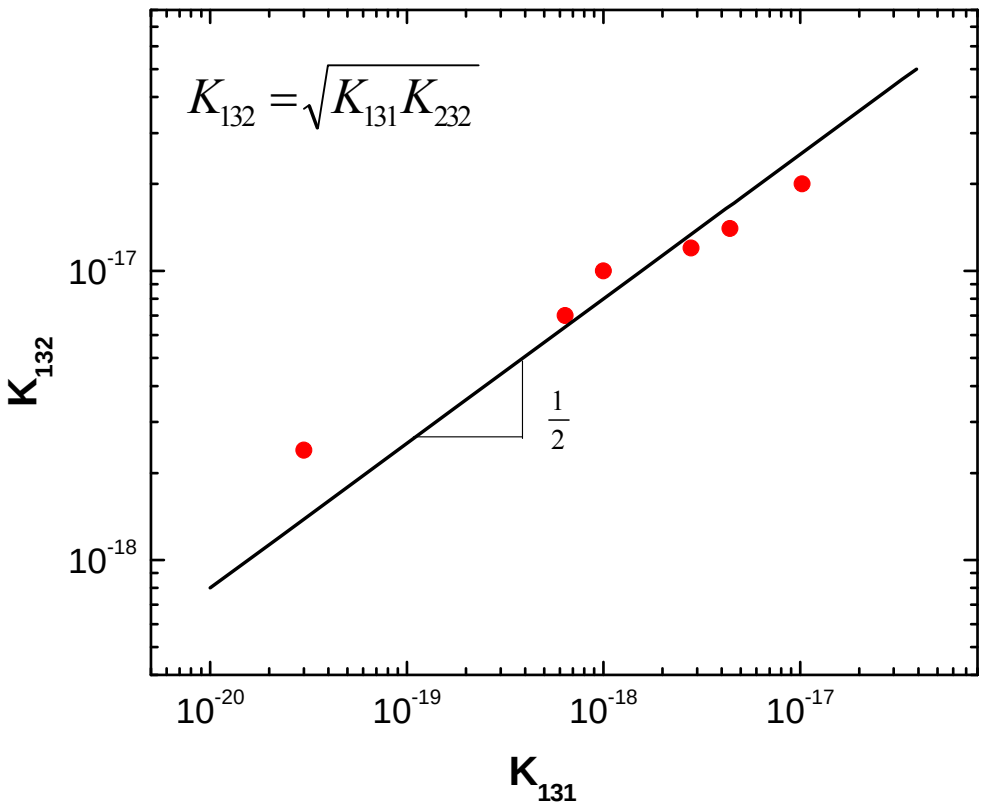

Figure 2.8 A plot of the asymmetric hydrophobic force constant (K_{132}) for wetting films *vs*. the square root of the symmetric hydrophobic force constant for the thin films between hydrophobic solid surfaces. Under condition that the slope is 0.5, one can determine the intercept of the plot numerically, which in turn gives $K_{232} = 5.3 \times 10^{-17}$ J. This value is close to the value reported in Ref. 60.

Table 2.1 The model parameters use to fit the data in Figure 8 to Eq. [2.1]

NaCl (M)	γ (mN/m)	R_f (mm)	Ψ_1[1] (mV)	Ψ_2[2] (mV)	κ^{-1} (nm)	K_{132} (J)
0	72.3	0.075	-40	-80	241	2.0×10^{-17}
10^{-5}	72.4	0.085	-43	-75	96.1	1.6×10^{-17}
10^{-4}	72.3	0.091	-47	-50	30.4	6.0×10^{-18}
10^{-3}	72.4	0.092	-47	-35	9.61	5.5×10^{-18}

[1]Ref. [62, 63]; [2]Present work

2.7 References

1. Yoon, R. H.; Mao, L. Q., Application of extended DLVO theory .4. Derivation of flotation rate equation from first principles. *Journal of Colloid and Interface Science* **1996,** 181, (2), 613-626.
2. Mao, L. Q.; Yoon, R. H., Predicting flotation rates using a rate equation derived from first principles. *International Journal of Mineral Processing* **1997,** 51, (1-4), 171-181.
3. Sulman, H. L.; Kirkpatrickpicard, H. E. Ore Concentration. 1905.
4. Derjaguin, B. V.; Kusakov, M. M., *Acta Physicochim. URSS* **1939,** 10, (1), 25-44.
5. Read, A. D.; Kitchener, J. A., Wetting films on silica. *Journal of Colloid and Interface Science* **1969,** 30, (3), 391-398.
6. Schulze, H. J., Die Instabilität dünner Flüssigkeitsfilme auf hydrophobierten Quarzoberflächen. *Colloid and Polymer Science* **1976,** 254, (4), 438-439.
7. Derjaguin, B. V.; Kusakov, M. M., *Acta Physicochim. URSS* **1939,** 10, (2), 153-174.
8. Derjaguin, B. V.; Churaev, N. V., Structural component of disjoining pressure. *Journal of Colloid and Interface Science* **1974,** 49, (2), 249-255.
9. Blake, T. D.; Kitchener, J. A., Stability of aqueous films on hydrophobic methylated silica. *J. Chem. Soc., Faraday Trans. 1* **1972,** 68, 1435-1442.
10. Stockelhuber, K. W.; Schulze, H. J.; Wenger, A., First Experimental Proof of the Nonexistence of Long-Range Hydrophobic Attraction Forces in Thin Wetting Films. *Chemical Engineering & Technology* **2001,** 24, (6), 624-628.
11. Pushkarova, R. A.; Horn, R. G., Bubble-solid interactions in water and electrolyte solutions. *Langmuir* **2008,** 24, (16), 8726-8734.
12. Schulze, H. J.; Stckelhuber, K. W.; Wenger, A., The influence of acting forces on the rupture mechanism of wetting films -- nucleation or capillary waves. *Colloids and Surfaces A: Physicochemical and Engineering Aspects* **2001,** 192, (1-3), 61-72.
13. Alexandrova, L.; Pugh, R. J.; Tiberg, F.; Grigorov, L., Confirmation of the heterocoagulation theory of flotation. *Langmuir* **1999,** 15, (22), 7464-7471.
14. Tchaliovska, S.; Herder, P.; Pugh, R.; Stenius, P.; Eriksson, J. C., Studies of the Contact Interaction between an Air Bubble and a Mica Surface Submerged in Dodecylammonium Chloride Solution. *Langmuir* **1990,** 6, (10), 1535-1543.
15. Mahnke, J.; Schulze, H. J.; Stckelhuber, K. W.; Radoev, B., Rupture of thin wetting films on hydrophobic surfaces: Part I: methylated glass surfaces. *Colloids and Surfaces A: Physicochemical and Engineering Aspects* **1999,** 157, (1-3), 1-9.
16. Churaev, N. V., Aqueous wetting films in contact with a solid phase. *Advances in Colloid and Interface Science* **2005,** 114-115, 3-7.
17. Israelachvili, J.; Pashley, R., The Hydrophobic Interaction Is Long-Range, Decaying Exponentially with Distance. *Nature* **1982,** 300, (5890), 341-342.
18. Christenson, H. K.; Claesson, P. M., Direct measurements of the force between hydrophobic surfaces in water. *Advances in Colloid and Interface Science* **2001,** 91, (3), 391-436.
19. Meyer, E. E.; Rosenberg, K. J.; Israelachvili, J., Recent progress in understanding hydrophobic interactions. *Proceedings of the National Academy of Sciences of the United States of America* **2006,** 103, (43), 15739-15746.
20. Christenson, H. K.; Claesson, P. M., Cavitation and the Interaction Between Macroscopic Hydrophobic Surfaces. *Science* **1988,** 239, (4838), 390-392.
21. Yaminsky, V. V.; Ninham, B. W., Hydrophobic force: lateral enhancement of subcritical fluctuations. *Langmuir* **1993,** 9, (12), 3618-3624.

22. Parker, J. L.; Claesson, P. M.; Attard, P., Bubbles, cavities, and the long-ranged attraction between hydrophobic surfaces. *The Journal of Physical Chemistry* **2002,** 98, (34), 8468-8480.
23. Tyrrell, J. W. G.; Attard, P., Atomic Force Microscope Images of Nanobubbles on a Hydrophobic Surface and Corresponding Force−Separation Data. *Langmuir* **2002,** 18, (1), 160-167.
24. Vinogradova, O. I., Drainage of a Thin Liquid Film Confined between Hydrophobic Surfaces. *Langmuir* **1995,** 11, (6), 2213-2220.
25. Vinogradova, O. I., Implications of Hydrophobic Slippage for the Dynamic Measurements of Hydrophobic Forces. *Langmuir* **1998,** 14, (10), 2827-2837.
26. Vinogradova, O. I., Slippage of water over hydrophobic surfaces. *International Journal of Mineral Processing* **1999,** 56, (1-4), 31-60.
27. Meyer, E. E.; Lin, Q.; Israelachvili, J. N., Effects of Dissolved Gas on the Hydrophobic Attraction between Surfactant-Coated Surfaces. *Langmuir* **2004,** 21, (1), 256-259.
28. Zhang, J. H.; Yoon, R. H.; Mao, M.; Ducker, W. A., Effects of degassing and ionic strength on AFM force measurements in octadecyltrimethylammonium chloride solutions. *Langmuir* **2005,** 21, (13), 5831-5841.
29. Wang, J. AFM Surface Force Measurements between Hydrophobized Gold Surfaces. PhD, Virginia Tech, Blacksburg, 2008.
30. Yoon, R. H.; Wang, J.; Eriksson, J. C., Thermodynamic Evidence for the molecular origin of hydrophobic force. *Science* **2009**.
31. Stockelhuber, K. W.; Radoev, B.; Wenger, A.; Schulze, H. J., Rupture of wetting films caused by nanobubbles. *Langmuir* **2004,** 20, (1), 164-168.
32. Sheludko, A., Thin liquid films. *Advances in Colloid and Interface Science* **1967,** 1, (4), 391-464.
33. Scheludko, A., *Proc. K. Ned Akad. Wet.* **1962,** B65, 76-87.
34. Laskowski, J.; Kitchener, J. A., The hydrophilic--hydrophobic transition on silica. *Journal of Colloid and Interface Science* **1969,** 29, (4), 670-679.
35. Platikanov, D., Experimental Investigation on the “Dimpling” of Thin Liquid Films. *J. Phys. Chem.* **1964,** 68, (12), 3619-3624.
36. Frankel, S. P.; Myseis, K. J., On the "dimpling" during the approach of two interfaces. *The Journal of Physical Chemistry* **1962,** 66, (1), 190-191.
37. Wang, L. G.; Yoon, R. H., Hydrophobic forces in thin aqueous films and their role in film thinning. *Colloids and Surfaces a-Physicochemical and Engineering Aspects* **2005,** 263, (1-3), 267-274.
38. Sharma, A.; Ruckenstein, E., Energetic criteria for the breakup of liquid films on nonwetting solid surfaces. *Journal of Colloid and Interface Science* **1990,** 137, (2), 433-445.
39. Sharma, A., Stability and Breakup of Thin Evaporating Water Films: Role of Hydrophobic Interaction. *Journal of Colloid and Interface Science* **1998,** 199, (2), 212-214.
40. Dimitrov, D. S.; Ivanov, I. B., Hydrodynamics of thin liquid films. On the rate of thinning of microscopic films with deformable interfaces. *Journal of Colloid and Interface Science* **1978,** 64, (1), 97-106.
41. Jain, R. K.; Ivanov, I. B., Thinning and Rupture of Ring-Shaped Films. *Journal of the Chemical Society-Faraday Transactions II* **1980,** 76, 250-266.
42. Maali, A.; Wang, Y.; Bhushan, B., Evidence of the No-Slip Boundary Condition of Water Flow between Hydrophilic Surfaces Using Atomic Force Microscopy. *Langmuir* **2009,** 25, (20), 12002-12005.
43. Lin, C.-Y.; Slattery, J. C., Thinning of a liquid film as a small drop or bubble approaches a solid plane. *Aiche Journal* **1982,** 28, (1), 147-156.

44. Sheludko, A., Exerowa, D., *Kolloid Z.* **1959,** 165, (148), 148.
45. Manica, R.; Connor, J. N.; Carnie, S. L.; Horn, R. G.; Chan, D. Y. C., Dynamics of Interactions Involving Deformable Drops: Hydrodynamic Dimpling under Attractive and Repulsive Electrical Double Layer Interactions. *Langmuir* **2007,** 23, (2), 626-637.
46. Hogg, R.; Healy, T. W.; Fuerstenau, D. W., Mutual coagulation of colloidal dispersions. *Trans. Faraday Soc.* **1965,** 62, 1638-1651.
47. Claesson, P. M.; Blom, C. E.; Herder, P. C.; Ninham, B. W., Interactions between water--stable hydrophobic Langmuir--Blodgett monolayers on mica. *Journal of Colloid and Interface Science* **1986,** 114, (1), 234-242.
48. Yoon, R. H.; Flinn, D. H.; Rabinovich, Y. I., Hydrophobic interactions between dissimilar surfaces. *Journal of Colloid and Interface Science* **1997,** 185, (2), 363-370.
49. Nedyalkov, M.; Alexandrova, L.; Platikanov, D.; Levecke, B.; Tadros, T., Wetting films on a hydrophilic silica surface obtained from aqueous solutions of hydrophobically modified inulin polymeric surfactant. *Colloid & Polymer Science* **2007,** 285, (15), 1713-1717.
50. Israelachvili, J., *Intermolecular & Surface Forces - 2nd Edition*. Academic Press: San Diego, 1992.
51. Monte, M. B. M.; Lins, F. F.; Oliveira, J. F., Selective flotation of gold from pyrite under oxidizing conditions. *International Journal of Mineral Processing* **1997,** 51, (1-4), 255-267.
52. Leja, J., *Surface chemistry of froth flotation* Plenum Press: New York, 1982.
53. Mielczarski, J. A.; Yoon, R. H., Fourier-Transform Infrared External Reflection Study of Molecular-Orientation in Spontaneously Adsorbed Layers on Low-Absorption Substrates. *Journal of Physical Chemistry* **1989,** 93, (5), 2034-2038.
54. Mielczarski, J. A.; Yoon, R. H., Spectroscopic Studies of the Structure of the Adsorption Layer of Thionocarbamate .1. On Copper and Activated Zinc-Sulfide. *Journal of Colloid and Interface Science* **1989,** 131, (2), 423-432.
55. Leppinen, J. O.; Basilio, C. I.; Yoon, R. H., Insitu Ftir Study of Ethyl Xanthate Adsorption on Sulfide Minerals under Conditions of Controlled Potential. *International Journal of Mineral Processing* **1989,** 26, (3-4), 259-274.
56. Leppinen, J. O.; Yoon, R. H.; Mielczarski, J. A., Ft-Ir Studies of Ethyl Xanthate Adsorption on Gold, Silver and Gold-Silver Alloys. *Colloids and Surfaces* **1991,** 61, 189-203.
57. Wang, J.; Yoon, R. H., Surface Forces Measured between Gold Substrates Hydrophobized by Spontaneous Adsorption of Short-Chain Xanthates. *Langmuir* **2009**.
58. Wang, J.; Yoon, R.-H., AFM Forces Measured between Gold Surfaces Coated with Self-Assembled Monolayers of 1-Hexadecanethiol. *Langmuir* **2008,** 24, (15), 7889-7896.
59. Christenson, H. K.; Fang, J.; Ninham, B. W.; Parker, J. L., Effect of divalent electrolyte on the hydrophobic attraction. *The Journal of Physical Chemistry* **1990,** 94, (21), 8004-8006.
60. Wang, L. G.; Yoon, R. H., Hydrophobic forces in the foam films stabilized by sodium dodecyl sulfate: Effect of electrolyte. *Langmuir* **2004,** 20, (26), 11457-11464.
61. Wang, L. G.; Yoon, R. H., Stability of foams and froths in the presence of ionic and non-ionic surfactants. *Minerals Engineering* **2006,** 19, (6-8), 539-547.
62. Li, C.; Somasundaran, P., Role of Electrical Double-Layer Forces and Hydrophobicity in Coal Flotation in Nacl Solutions. *Energy & Fuels* **1993,** 7, (2), 244-248.
63. Li, C.; Somasundaran, P., Reversal of bubble charge in multivalent inorganic salt solutions--Effect of magnesium. *Journal of Colloid and Interface Science* **1991,** 146, (1), 215-218.
64. van Oss, C. J., *Interfacial Forces in Aqueous Media - 2nd Edition*. CRC Press: Boca Raton, 2006.
65. Du, Q.; Freysz, E.; Shen, Y. R., Surface Vibrational Spectroscopic Studies of Hydrogen Bonding and Hydrophobicity. *Science* **1994,** 264, (5160), 826-828.

66. Scatena, L. F.; Brown, M. G.; Richmond, G. L., Water at Hydrophobic Surfaces: Weak Hydrogen Bonding and Strong Orientation Effects. *Science* **2001,** 292, (5518), 908-912.
67. Lauga, E., Microfluidics: The No-Slip Boundary Condition. In *Handbook of Experimental Fluid Dynamics*, Tropea, C.; Yarin, A.; Foss, J. F., Eds. Springer: New York, 2007; pp 1219-1240.
68. Angarska, J. K.; Dimitrova, B. S.; Danov, K. D.; Kralchevsky, P. A.; Ananthapadmanabhan, K. P.; Lips, A., Detection of the hydrophobic surface force in foam films by measurements of the critical thickness of the film rupture. *Langmuir* **2004,** 20, (5), 1799-1806.
69. Berthelot, D., *Compt. rend.* **1898,** 126, 1703-1857.
70. Eriksson, J. C.; Yoon, R. H., Hydrophobic Attraction in the Light of Thin Film Thermodynamics. In *Colloid Stability -The Role of Surface Forces, Colloid and Interface Science Series*, Tadros, T. F., Ed. Wiley-VCH: 2006; pp 99-131.

Chapter 3

Thinning and Rupture of Wetting Film on Silica Plate in the $C_{18}TACl$ Aqueous Solution

Abstract

Thin Film Balance (TFB) technique is employed to measure the thinning kinetics and critical rupture thickness of dimpled wetting film on a silica plate in $C_{18}TACl$ aqueous solution. Assuming the immobile surface at the air/water interface and no hydrodynamic pressure at the barrier rim of dimpled film, the thinning of wetting film is controlled by the sum of the capillary pressure and disjoining pressure. The kinetics of wetting film thinning is, therefore, viewed as Reynolds lubrication theory when only considering the thinning of wetting film at the rim of film. It is found that thinning kinetics of film on silica plate in $C_{18}TACl$ aqueous solution could be predicted only when considering the extra attractive forces named as "hydrophobic forces", since van der waals forces and electrostatic forces both are repulsive. The values of hydrophobic forces constant (K_{132}) varies with different concentration of $C_{18}TACl$ and different immersion time. At $5x10^{-6}$ M $C_{18}TACl$ aqueous solution, K_{132} reaches the maximum for 1 hour which is consistent with the contact angle measurement. The effect of electrolyte on kinetics of wetting film thinning and critical rupture thickness is also examined. The critical rupture thickness (H_r) and hydrophobic forces constant (K_{132}) decreases with increasing the NaCl concentration, probably because of the compression of electrostatic double layer forces and decrease of hydrophobic forces. It is, therefore, suggested that hydrophobic forces plays a vital role in destabilizing the wetting film between air bubbles and hydrophobic particles.

3.1 Introduction

Froth Flotation has been used for more than 100 years for separating different minerals from each other since 1905, when the air bubble was first used for flotation.[1] The basic principle of froth flotation is rendering the target minerals hydrophobic and unselected minerals hydrophilic to achieve the separation of minerals, and therefore, the attachment between the air bubble and hydrophobic particles is the fundamental process for successful flotation. The attachment between air bubble and hydrophobic particles involves three sub-processes: 1) air bubble approaches the particles by hydrodynamics; 2) the thinning of wetting film between air bubble and particles; 3) rupture of wetting film to form the three-phase froth. Many investigators attempted to model the flotation process by hydrodynamics parameters without considering any surface forces. In most flotation condition, however, both the van der Waals forces and electrostatic double layer forces are repulsive, which give no driving forces for thinning and rupture of wetting film on hydrophobic particles[2]. It appears, therefore, the interaction between the bubbles and particles are the key for modeling the flotation process.

Derjaguin and Duhkin[3] were the first to introduce the surface forces to investigate the bubble-particles interaction, but they only considered van der Waals and electrostatic forces. It was till 1968 that Laskowski and Kitchener[4] found that the water films of a certain film thickness on the methylated silica surface were unstable and the wetting film would rupture spontaneously, while both double-layer and dispersion forces were repulsive. Blake and Kitchener[5] later found that the rupture thickness of wetting film on methylated silica was 60 to 220 nm, which indicated that the thin water film on methylated silica was unstable due to the presence of a "long-range" attractive forces. More recently, Israelachvili and pashley[6, 7] firstly measured the long-range attractive forces (or hydrophobic forces) between two macroscopic surfaces in CTAB solution using Surface Forces Apparatus (SFA). Other investigators[8-10] also measured attractive hydrophobic forces between two hydrophobic surfaces using Atomic Force Microscope (AFM).

The drainage and rupture of wetting film studied by Thin Film Balance (TFB) technique also showed evidences of existence of hydrophobic forces in wetting film. Tchalivska et al., [11]investigated the wetting properties of hydrophobic mica in dodecyl ammonium chloride (DAC) solution, and found that hydrophobic attraction forces played a vital role in thin-film lifetimes as well as the rates of expansion of the meniscus perimeter. The papers[2, 10, 12, 13] published by Yoon et al. suggested that thinning and rupture of thin water film intervened by hydrophobic surfaces must include the influence of hydrophobic attractive forces.

The discussion of existence of hydrophobic attraction forces on the wetting film, however, did not turn out a well-accepted explanation. Schulze et al.,[14, 15] suggested that gas bubble at heterogeneities of solid surfaces was responsible for the rupture of wetting film on methylated silica without considering any long-range hydrophobic attraction, yet they ignored the slight difference on slope of kinetics of wetting film thinning. Mahnke et al.[16] observed a hole in the dimpled wetting film on hydrophobic glass surfaces coated with fatty acid Langmuir-Blodgett layers, and they indicated that nucleation of the air bubble is the reason for the high rupture thickness. Stckelhuber et al.,[17, 18]recently proposed that nanobubble on the hydrophobic solid

surface can be the cause of rupture of wetting films without considering any surface forces acting on the interface.

In the present work, kinetics of wetting film thinning on the silica surface in C_{18}TACl solution was studied using Scheludko cell[19] by TFB[2, 12, 13] techniques. Assuming the immobile surface at liquid/vapor interface and no hydrodynamic pressure at the barrier rim of dimpled film, film drainage at the barrier rim was viewed as satisfying the Reynolds lubrication theory[20-22]. The result was analyzed using the Reynolds equation to determine the hydrophobic forces constant K_{132} as function of C_{18}TACl and electrolyte (NaCl) concentration. The origin of long-range hydrophobic forces in the wetting films was discussed.

3.2 Experimental Details

Octadecyltrimethylammonium chloride (C_{18}TACl, 97%) was obtained from TCI America without any purification. Sodium chloride (99.999%, Sigma-Aldrich) was used as electrolyte. It is further roasted in furnace at 500°C for six hours to remove the organic impurity. Milipore water was obtained by Direct-Q 3 water purification system with the resistivity of 18.2 MΩ/cm. H_2SO_4 (98%ACS, Fisher Scientific) and H_2O_2 (29-32%, Alfa Aesar) was received without any treatment. The C_{18}TACl aqueous solution was prepared newly before each experiment to prevent the adsorption of surfactants on the glassware. Polished Fused quartz (Technical Glass Product, Inc) was boiled in a piranha solution (7:3 volume% H_2SO_4/H_2O_2) for 1 hours. The plate is rinsed with pure water ultrasonically for 30min, and then dried in a nitrogen gas stream.

The kinetics of film thinning between air bubble and plate is measured by Thin Film Balance (TFB) technique developed by Scheludko and Exerowa[23]. The original design is to measure the thickness of soap films between two air bubbles as function of time[19], while we use this technique to measure the film thickness of wetting film between air bubble and flat plate as function of time in the present work. The inner radius of the film holder (R_c) is 2.0 mm. The plates are placed on the top of film holder in liquid prior to each experiment, to make sure that there is no observable air bubble attached on the plate in the film holder. The whole cell is then placed on an inverted microscopic stage (Olympus IX51). Halogen Lamp (100W, Osram) is used as light sources for the microscope, and the band-pass filter (NT46-053, Edmund Optics) is placed after the light sources to get the monochromic green light with center wavelength of 526 nm. The initial thinning of wetting film above the 1000 nm is by squeezing liquid out by pistons. To capture the changing thinning process of wetting film in several seconds, the monochromic interference images are recorded by high speed CCD camera (Fastcam 512PCI, Photron), and from which the changing profile of wetting film is obtained using the microinterferometric technique by programming in Matlab.

The surface tension isotherms of C_{18}TACl solution at low concentration in absence and presence of NaCl are measured using Wilhelmy-plate method. The platinum that we use in experiment is assumed perfect hydrophilic. The surface tension of pure water that we use at room temperature is 72.3 mN/m.

Advanced, receding and equilibrium contact angle are measured on the gold plates by the sessile drop method using a contact angle goniometer (Ramé-Hart, Inc.) under ambient conditions. The test liquid for contact angle measurement is pure water.

3.3 Result and Discussion

Fig. 3.1 shows the changing film profile of wetting film between air bubble and polished quartz plate in 10^{-1} M NaCl solution as the function of the radial position of film (r) and time (t). As described in previous literatures[13], the drainage of thin water film on the flat solid surface is initially controlled by capillary pressure at the separation distance of above 500 nm. As the gas bubble approaches the flat solid surface, the "dimple" will form due to viscous liquid drag. Once a "dimple" is formed, the liquid inside dimple is entrapped by a thinner "barrier ring". The initial time (0 s) noted in Fig. 3.1 is a reference time at certain separation film thickness, instead of initial time of dimpled film formation. The wetting film is thinning gradually and does not rupture up to 31 s.

Fig. 3.2 shows the film thickness as function of time in 10^{-1} M NaCl solution at the center and at the barrier rim. It is known that the electrostatic double layers forces between two macroscopic surfaces are screened at high concentration of electrolyte solution. At 25°C, the Debye length of aqueous NaCl solution can be given as follows[24]:

$$\kappa^{-1} = \frac{0.314}{\sqrt{C_{NaCl}}} \ (nm) \tag{3.1}$$

At 10^{-1} M NaCl solution, the Debye length (κ^{-1}) is 0.96 nm, which indicates that the double layer forces do not need to be considered in DLVO theory. The drainage of wetting film is, therefore, only controlled by the capillary pressure and dispersion forces. It is reported[21] that the drainage of wetting film at the barrier ring proximately satisfies the Reynolds lubrication approximation, which is derived from drainage of liquid between two flat discs. Thus the drainage rate of wetting film is given by following equation:

$$-\frac{dH}{dt} = \frac{2H^3\Delta P}{3\mu R_f^2} \tag{3.2}$$

where H is film thickness, t is drainage time, μ is the bulk viscosity, R_f is the film radius up to the barrier rim of film and ΔP is the excess pressure for film thinning. Since the electrostatic double layer forces is negligible at high concentration of NaCl solution, the driving pressure of film thinning is given as follows:

$$\Delta P = \frac{2\sigma}{R} - \Pi_{\mathrm{vdW}} - \frac{\sigma}{r}\frac{\partial}{\partial r}\left(r\frac{\partial h}{\partial r}\right) \tag{3.3}$$

where R is the radius of film holder, σ is the surface tension of liquid, Π_{vdW} is the disjoining pressure contributed by van der Waals dispersion forces and $\frac{\sigma}{r}\frac{\partial}{\partial r}\left(r\frac{\partial h}{\partial r}\right)$ is the hydrodynamic pressure term due to the local curvature of film. It is shown that the theoretical model by Reynolds equation successfully predicts the thinning kinetics of wetting film at the rim of film without considering any hydrodynamic pressure. The thinning rate at the center of film is slower than that at the barrier rim of film, mainly due to the hydrodynamic repulsive pressure resisting the thinning of film at the center.

Fig. 3.3 shows comparison of changing film profile of wetting film on the polished quartz surface in the pure water (Fig. 3a) and in the $5x10^{-6}$ M $C_{18}TACl$ solution (Fig. 3b) for 10 minutes after film formation. Since the initial drainage of wetting film is only driven by the capillary pressure, we set the reference time t=0 s after the "dimple" is formed. In the pure water, the wetting film is thinning gradually and reaches the equilibrium film thickness ($H_e \approx 130$ nm), at which the disjoining pressure equates to the capillary pressure, as shown in Fig. 3a. However the wetting film on the quartz surface in the $5x10^{-6}$ M $C_{18}TACl$ solution for 10 min is thinning much faster than those in the pure water, as shown in Fig. 3b. The thin film only takes 0.48 s to rupture since the formation of initial "dimpled" film, while the wetting film in the pure water does not rupture in the infinite time. The thinning of wetting film at the center of film is much slower than that at the barrier rim of film in the $5x10^{-6}$ M $C_{18}TACl$ solution, due to the strong attractive surface forces between gas bubble and flat hydrophobic surface inducing liquid drag at the solid/liquid interface.

Assuming no hydrodynamic pressure acting at the barrier rim of film, the film thinning is controlled by disjoining pressure and capillary pressure, as discussed above. The comparison of thinning curve of wetting film at the barrier rim in the pure water and in the $5x10^{-6}$ M $C_{18}TACl$ solution for 10 min is shown in Fig. 3.4. The solid line represents the theoretical prediction of film thinning at the rim of film by Reynolds equation, which is exactly agrees with experimental date of wetting film thinning in the pure water, while it failed to predict the wetting film drainage in $5x10^{-6}$ M $C_{18}TACl$ solution if not considering any attractive forces contributing to DLVO theory. Thus it is necessary to propose that there is another attractive disjoining pressure causing the faster thinning rate of wetting film. Tchalivska et al. [11] and Yoon[2] suggested that hydrophobic forces should be the driving forces for attachment of air bubbles and hydrophobic particles.

It is proposed that hydrophobic forces induce the unpredicted faster thinning kinetics of wetting film on quartz surface in $C_{18}TACl$ aqueous solution. Fig. 3.5 shows the kinetics curve of wetting film at the barrier rim in $5x10^{-6}$ M $C_{18}TACl$ solution for 30 min. The film radius of dimpled film is 0.11 mm. The dotted line stands for the Reynolds equation prediction without considering hydrophobic forces, while the solid line stands for the Reynolds equation prediction corrected by the hydrophobic forces. In $5x10^{-6}$ M $C_{18}TACl$ solution, the silica surface reaches the point of ξ-potential reversal[25], and thus, the electrostatic double layer forces is negligible. The fitting hydrophobic forces constant $K_{132}=3.3x10^{-17}$ J, which is two thousand times larger than Hamaker constant ($A_{132}=1.13x10^{-20}$ J). The deviation between experimental date and corrected Reynolds prediction at the separation distance below the 200 nm is probably due to the heterogeneous thinning of wetting film.

Fig. 3.6 shows microinterferometric images of wetting film on the silica surface in $5x10^{-6}$ M $C_{18}TACl$ solution before rupture to explain the heterogeneous drainage. The reference time (0 s) is set for comparing the images in different time interval. As shown in Fig 3.6, there exists a distinct point at the barrier rim of film which indicates that the film thickness at this point is much thinner compared with surroundings. Thus the thin water film on the silica surface in $C_{18}TACl$ aqueous solution collapses at specific point of barrier ring. Different from the relatively uniform coating of potassium amyl xanthate (PAX) on the gold due to chemical bonding between S atom of PAX molecule and gold palte as described in previous chapter, the $C_{18}TA^+$ ions are more likely form cluster on the quartz isolated. Zhang et al. [26]observed that cluster is formed on the quartz surface in the $C_{18}TACl$ aqueous solution by AFM. Therefore, the jump phenomenon on the draining thin film is probably due to the cluster formation on the quartz surface in $C_{18}TACl$ aqueous solution.

The effect of the immersion time on the thinning rate of wetting film in $5x10^{-6}$ M $C_{18}TACl$ solution is studied, as shown in Fig. 3.7. The radius of film is around 0.115 mm, and surface tension of aqueous solution is 66 mN/m. It is shown that the critical rupture thickness of wetting film is nearly same for different immersion time, while the thinning rate strongly depends on the immersion time. At the immersion time of 10 min, the kinetics of film thinning is fastest and hydrophobic forces constant $K_{132} = 3.4x10^{-17}$ J. As the immersion time increases from 10 min to 100 min, the thinning rate becomes slower and corresponding hydrophobic forces constant K_{132} decreases to$1.2x10^{-17}$ J when the immersion time is 100 min. It may be attributed to the formation of multilayer of surfactants on the silica surface which reduces the hydrophobicity of surface.

Fig. 3.8 shows the thinning kinetics of wetting film on the silica surface in different concentration of $C_{18}TACl$ aqueous solution for 60 minutes. The fitting parameters to determine the hydrophobic forces are shown in Table 3.1. The increase of zeta potential on the air/water interface is due to the adsorption of $C_{18}TA^+$ ions onto the air/water interface. The reversal of zeta-potential on the solid/liquid interface above the $5x10^{-6}$ M for $C_{18}TACl$ solution results in the attractive electrostatic double layer forces. It is probably due to the flip-flop orientation of $C_{18}TA^+$ surfactants on the silica surface with the positive ions toward the liquid phase. However, the total disjoining pressure contributed from both dispersion forces and attractive electrostatic double layer forces still fails to predict the faster drainage rate of wetting film in $C_{18}TACl$ aqueous solution. At the $5x10^{-6}$ M $C_{18}TACl$, the hydrophobic forces is strongest with the hydrophobic forces constant $K_{132}=3.5x10^{-17}$ J. At $1x10^{-5}$ M $C_{18}TACl$ solution, the hydrophobic forces decreases probably due to the reversal orientation of $C_{18}TA^+$ molecules on the quartz plate, which reduces the hydrophobicity of solid. At the low concentration of $C_{18}TACl$ solution, the drainage rate of wetting film is relatively slow with hydrophobic forces constant $K_{132}=1x10^{-17}$ J at $2x10^{-6}$ M $C_{18}TACl$ solution.

According to Dupre's equation, the change in the free energy due to the replacement of the solid-liquid interface by solid-gas interface is given by:

$$\Delta G = \gamma_{SG} - (\gamma_{SL} + \gamma_{LG}) \qquad [3.4]$$

Combined with Young's equation, the Dupre's equation could be rewritten as follows:

$$\Delta G = \gamma_{LG}(\cos\theta - 1) \quad [3.5]$$

It is obvious that the free energy associated with bubble-particle attachment is dependent on contact angle on the solid surface. The higher the contact angle is, the more likely the bubble attaches the particles. Fig. 3.9 shows the correlation between the lifetime (t_{lt}) of wetting film after the film formation and receding contact angle (θ_r) at various low concentration of C_{18}TACl solution. In the present work, the liquid is sucking out due to the capillary pressure, and thus, the drainage rate is more correlated to the receding contact angle instead of advanced contact angle. As shown in Fig. 3.9, high contact angle relates to the short lifetime of wetting film. At $5x10^{-6}$ M C_{18}TACl solution, receding contact angle is 66 ^{o} and film lifetime is around 0.4 s. As the C_{18}TACl concentration increases or decreases, the lifetime of film increases while the receding contact angle decreases. Thereby, contact angle relates to the attachment of air bubbles and particles and following floatability of minerals.

In Fig. 3.10, the effect of electrolyte (NaCl) concentration on the kinetics of wetting film drainage in an air-equilibrium $5x10^{-6}$ M C_{18}TACl solution is shown. The surface potential (zeta potential here we used to represent the surface potential) of plate in aqueous C_{18}TACl solution that used to calculate the hydrophobic constant is obtained by experiment. As the electrolyte concentration increases, electrostatic double layer forces between air bubble and solid plate are screened. Also the hydrophobic forces decrease with increases of electrolyte concentration. At $3x10^{-3}$ M NaCl solution, the wetting film does not rupture up to 11 s. Hydrophobic forces constant K_{132} decreases from $2x10^{-17}$ J without electrolyte to $6x10^{-19}$ J at $3x10^{-3}$ M NaCl solution. Fig. 11shows the critical film thickness and lifetime of film of wetting film in $5x10^{-6}$ M C_{18}TACl solution as a function of NaCl concentration. It is shown that the critical film thickness decreases as the electrolyte concentration increases. It is probably because both electrostatic double layer forces and hydrophobic forces decrease with increasing the electrolyte concentration. Thus the only driving forces for wetting film thinning is capillary pressure, which is not enough to introduce the surface wave to induce the rupture of wetting film.

3.4 Conclusion

Reynolds equation is illustrated to predict the thinning kinetics of wetting film at the barrier ring of film. By assuming negligible influence from the slippage on the solid/liquid interface, the kinetics curve of wetting film drainage on hydrophobic forces is fitted by Reynolds equation corrected by considering the hydrophobic forces.

Film profile on the hydrophilic surface and on the hydrophobic surface is compared. Wetting film on the hydrophilic surface is thinning gradually and stabilizes at certain film thickness, while wetting film on the hydrophobic surface ruptures spontaneously with large dimple shape due to the strong attractive forces. The rupture of wetting film on the silica surface in C_{18}TACl aqueous solution is heterogeneous, probably because of the cluster formation of $C_{18}TA^+$ cationic surfactants on silica surface.

The result obtained in the present work shows that the long-range hydrophobic forces are observed between the air bubble and silica plate in C_{18}TACl solution. The hydrophobic force is dependent on the concentration of C_{18}TACl solution and the immersion time. The calculated hydrophobic forces constant K_{132} is correlated to contact angle, which also suggests that the hydrophobic forces are corresponding to the probability of bubble-particle attachment. It is also shown that the hydrophobic forces diminish as increase of electrolyte concentration, probably because the origin of hydrophobic forces is ordered water structure in vicinity of hydrophobic surface.

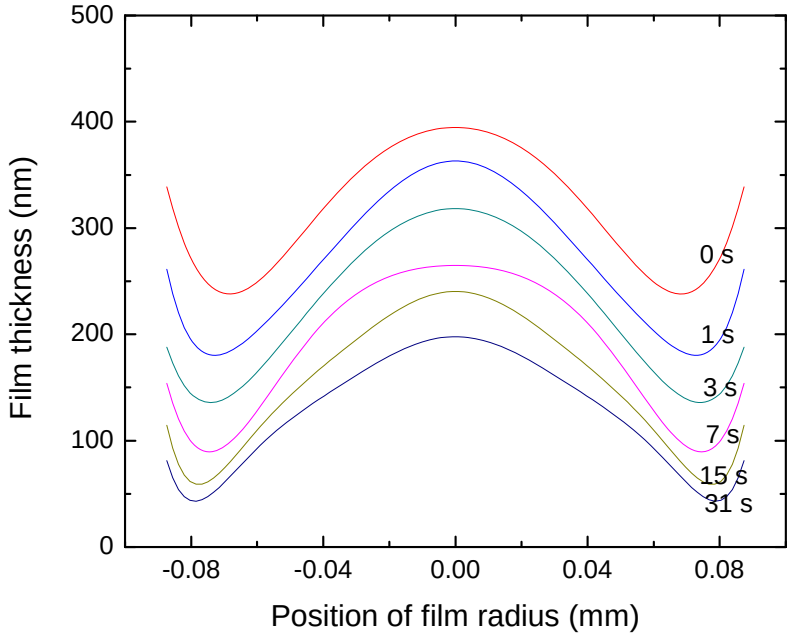

Figure 3.1 The time-changing film profile of wetting film formed on a polished quartz plate in 10^{-1} M NaCl solution

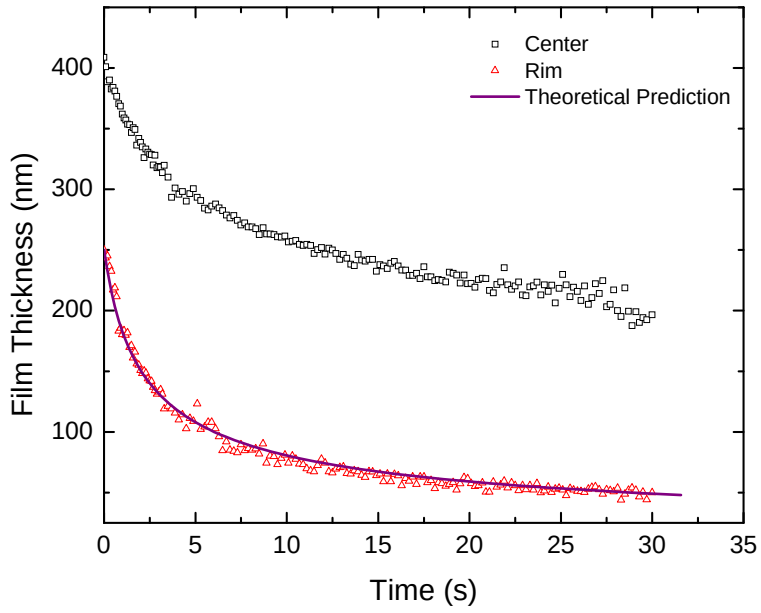

Figure 3.2 Thinning kinetics curve of wetting film in 10^{-1} NaCl solution at the center (open square) and at the barrier rim of film (open triangular). The blue line represents the theoretical prediction by Reynolds equation without considering hydrodynamic pressure.

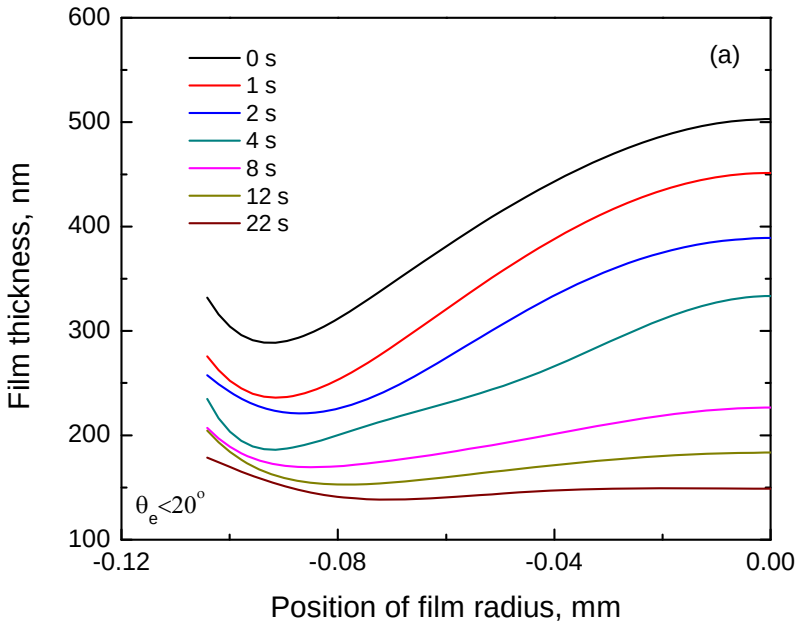

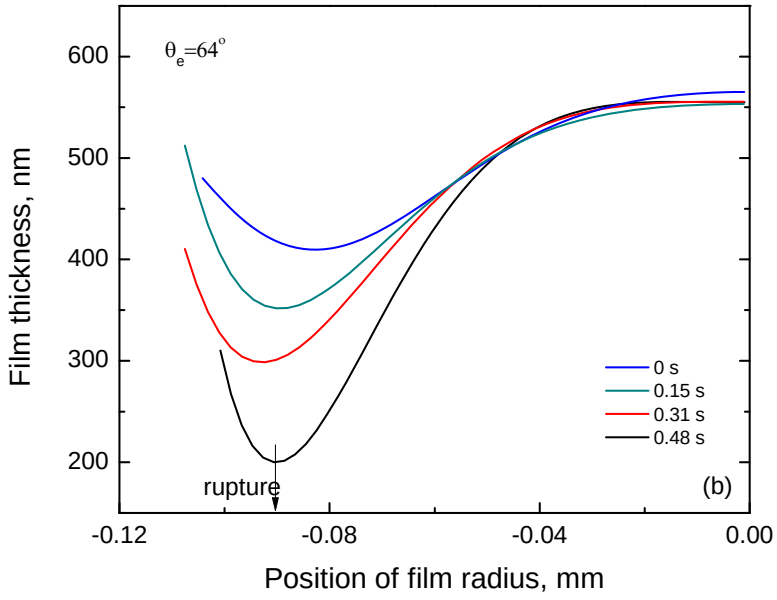

Figure 3.3 Comparison of time-changing profile of wetting film formed on a quartz surface in the pure water (Fig. 3a) and in the $5x10^{-6}$ M $C_{18}TACl$ solution (Fig. 3b) with contact time of 10 minutes.

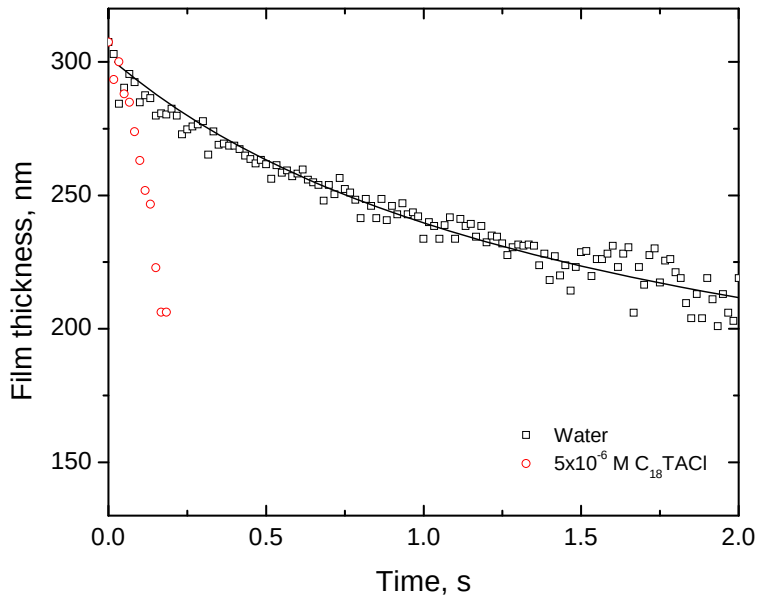

Figure 3.4 Changes in thickness of wetting film formed on a quartz surface in the pure water (open square) and in the $5x10^{-6}$ M $C_{18}TACl$ solution with contact time of 10 minutes (open circle). The solid line represents theoretical prediction of film thinning at the rim of film by Reynolds equation.

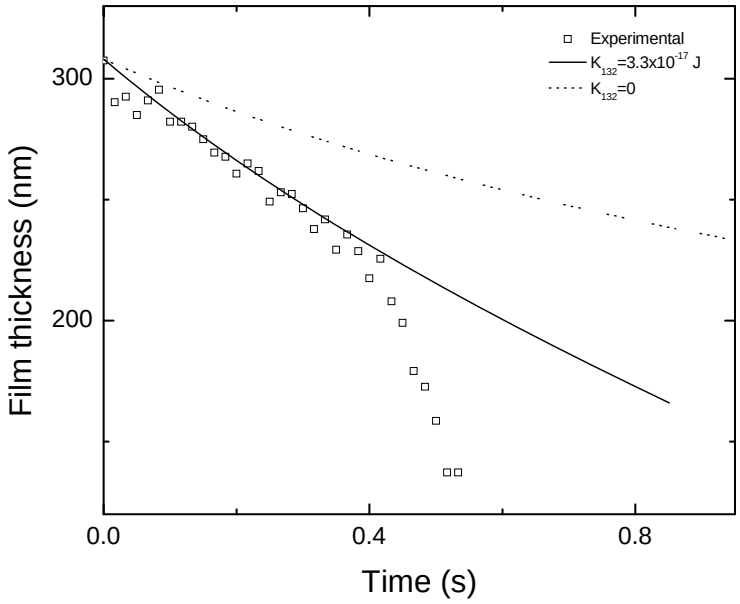

Figure 3.5 Kinetics curve of film thinning in an air-equilibrated 5x10^{-6} M C_{18}TACl solution with the contact time of 30 minutes. The solid line represents the theoretical prediction by Reynolds equation with considering the hydrophobic forces, while the dotted line stands for theoretical prediction by Reynolds equation without considering the hydrophobic forces.

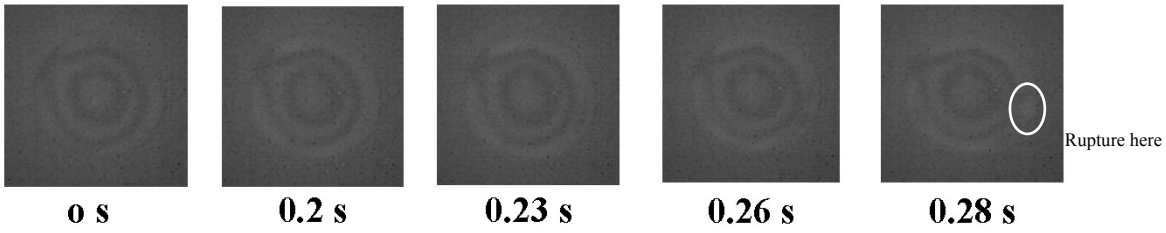

Figure 3.6 Microinterferometric images of wetting film formed on a quartz surface in 5x10^{-6} M C_{18}TACl solution with contact time of 10 minutes.

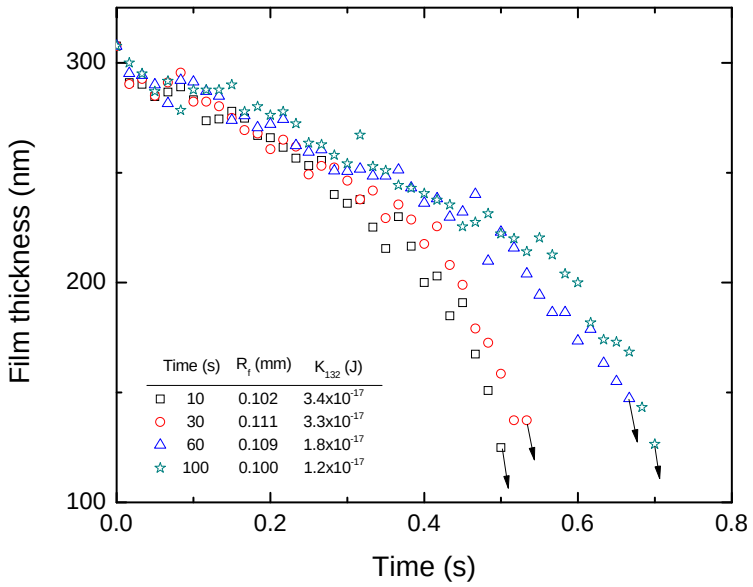

Figure 3.7 Effect of contact time on thinning kinetics curve of wetting film formed on a quartz plate in an air-equilibrated $5x10^{-6}$ M $C_{18}TACl$ solution.

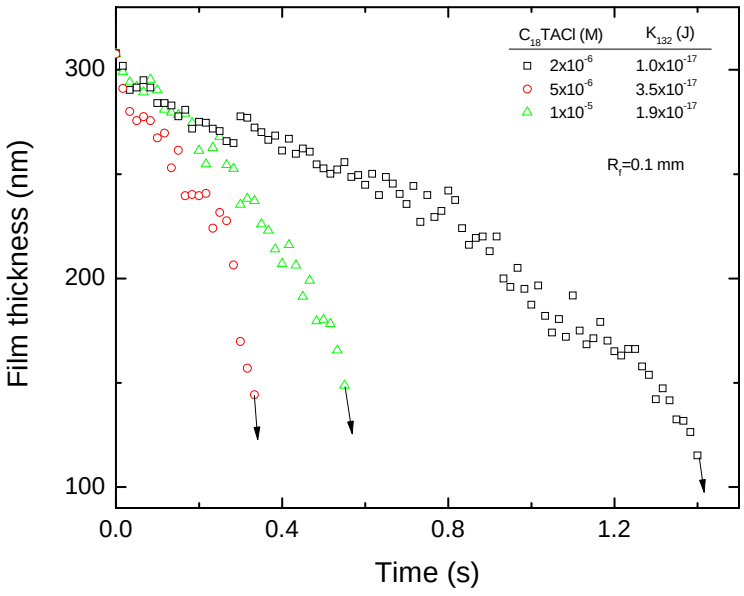

Figure 3.8 Effect of concentration of $C_{18}TACl$ solution on wetting film drainage on a quartz plate in an air-equilibrium $C_{18}TACl$ solution with the contact time of 60 minutes.

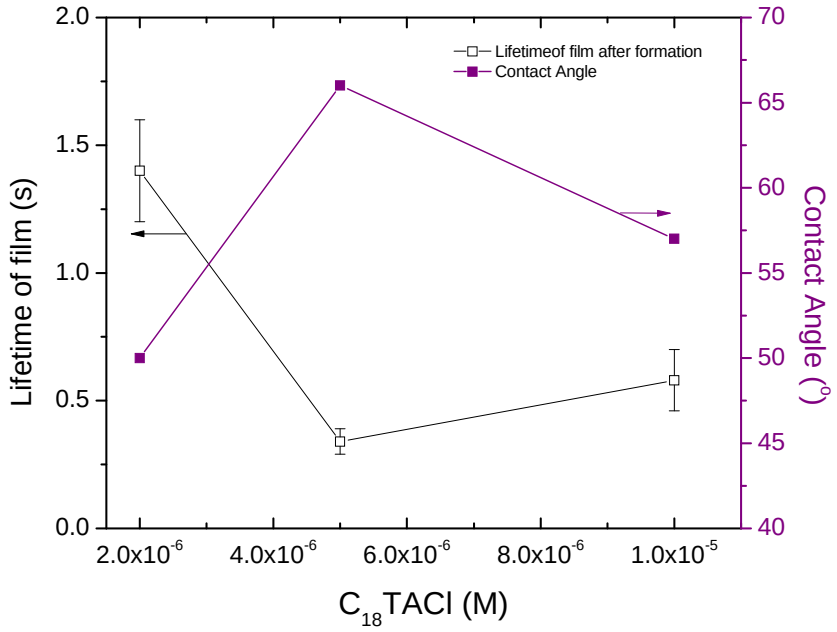

Figure 3.9 Correlation between lifetime of wetting film after film formation and equilibrium contact angle

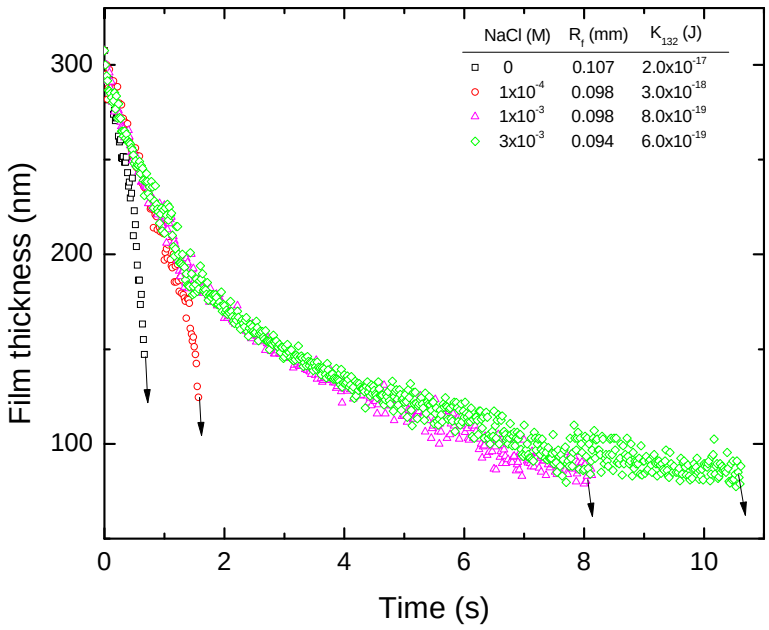

Figure 3.10 Effect of electrolyte (NaCl) on thinning kinetics of wetting film formed on a quartz plate in an air-equilibrated $5x10^{-6}$ M $C_{18}TACl$ solution with the contact time of 60 minutes.

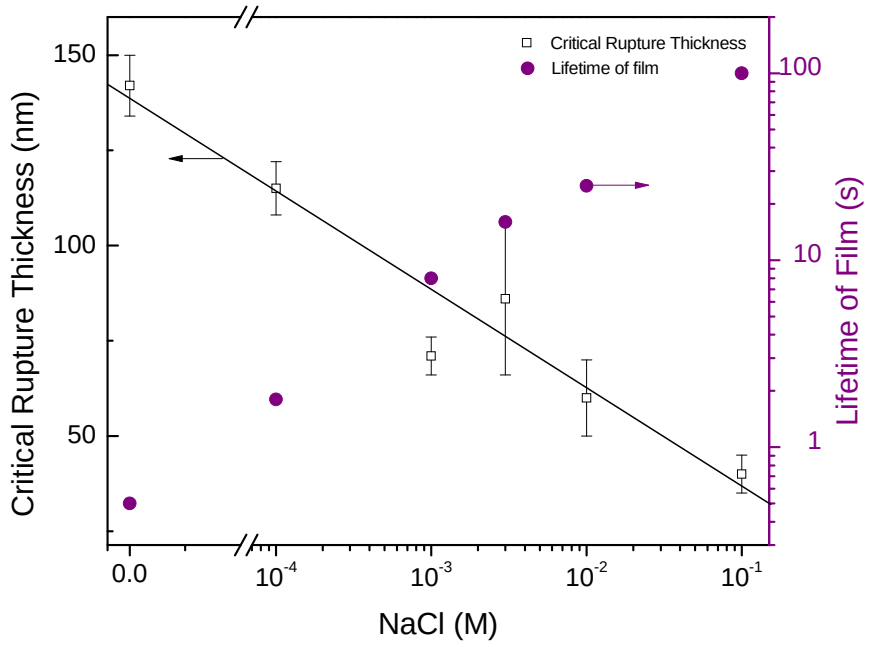

Figure 3.11 Effect of electrolyte (NaCl) on critical rupture thickness (open square) and lifetime of wetting film (solid circle) on a quartz plate in an air-equilibrated $5x10^{-6}$ M $C_{18}TACl$ solution. The solid line represents the trend of decreasing critical thickness as function of the concentration of electrolyte.

Table 3.1 Fitting parameters in an air-equilibrium $C_{18}TACl$ aqueous solution

$C_{18}TACl$ (M)	γ (mN/m)	Φ_{air} [1] (mV)	Φ_{plate} [2] (mV)	κ^{-1} (nm)	A_{132} (J)	K_{132} (J)
$2x10^{-6}$	67.9	-80	-30	214	$-1.13x10^{-20}$	$1.0x10^{-17}$
$5x10^{-6}$	66.0	0	10	136	$-1.13x10^{-20}$	$3.5x10^{-17}$
$1x10^{-5}$	56.3	30	48	96.1	$-1.13x10^{-20}$	$1.9x10^{-17}$

1. Literature 2. Literature[27]

3.5 References

1. Fuerstenau, D. W., A Century of Developments in the Chemistry of Flotation Processing. **2007**, 61.

2. Yoon, R. H., The role of hydrodynamic and surface forces in bubble-particle interaction. *International Journal of Mineral Processing* **2000,** 58, (1-4), 129-143.

3. Dukhin, B. V. D. S. S., Theory of flotation of small and medium-size particles. *Institution of Mining and Metallurgy* **1961,** 70.
4. Laskowski, J.; Kitchener, J. A., The hydrophilic--hydrophobic transition on silica. *Journal of Colloid and Interface Science* **1969,** 29, (4), 670-679.
5. Blake, T. D.; Kitchener, J. A., Stability of aqueous films on hydrophobic methylated silica. *J. Chem. Soc., Faraday Trans. 1* **1972,** 68, 8.
6. Pashley, R. M.; Israelachvili, J. N., A comparison of surface forces and interfacial properties of mica in purified surfactant solutions. *Colloids and Surfaces* **1981,** 2, (2), 169-187.
7. Israelachvili, J.; Pashley, R., The Hydrophobic Interaction Is Long-Range, Decaying Exponentially with Distance. *Nature* **1982,** 300, (5890), 341-342.
8. Wang, J.; Yoon, R.-H., AFM Forces Measured between Gold Surfaces Coated with Self-Assembled Monolayers of 1-Hexadecanethiol. *Langmuir* **2008,** 24, (15), 7889-7896.
9. Yoon, R. H.; Ravishankar, S. A., Long-range hydrophobic forces between mica surfaces in dodecylammonium chloride solutions in the presence of dodecanol. *Journal of Colloid and Interface Science* **1996,** 179, (2), 391-402.
10. Yoon, R. H.; Flinn, D. H.; Rabinovich, Y. I., Hydrophobic interactions between dissimilar surfaces. *Journal of Colloid and Interface Science* **1997,** 185, (2), 363-370.
11. Tchaliovska, S.; Herder, P.; Pugh, R.; Stenius, P.; Eriksson, J. C., Studies of the contact interaction between an air bubble and a mica surface submerged in dodecylammonium chloride solution. *Langmuir* **1990,** 6, (10), 1535-1543.
12. Yoon, R. H.; Aksoy, B. S., Hydrophobic forces in thin water films stabilized by dodecylammonium chloride. *Journal of Colloid and Interface Science* **1999,** 211, (1), 1-10.
13. Wang, L. G.; Yoon, R. H., Hydrophobic forces in thin aqueous films and their role in film thinning. *Colloids and Surfaces a-Physicochemical and Engineering Aspects* **2005,** 263, (1-3), 267-274.
14. K. W. Stockelhuber, H. J. S., A. Wenger,, First Experimental Proof of the Nonexistence of Long-Range Hydrophobic Attraction Forces in Thin Wetting Films. *Chemical Engineering & Technology* **2001,** 24, (6), 624-628.
15. Schulze, H. J.; Stokelhuber, K. W.; Wenger, A., The influence of acting forces on the rupture mechanism of wetting films -- nucleation or capillary waves. *Colloids and Surfaces A: Physicochemical and Engineering Aspects* **2001,** 192, (1-3), 61-72.
16. Mahnke, J.; Schulze, H. J.; Stckelhuber, K. W.; Radoev, B., Rupture of thin wetting films on hydrophobic surfaces. Part II: fatty acid Langmuir-Blodgett layers on glass surfaces. *Colloids and Surfaces A: Physicochemical and Engineering Aspects* **1999,** 157, (1-3), 11-20.
17. Stockelhuber, K. W.; Radoev, B.; Wenger, A.; Schulze, H. J., Rupture of wetting films caused by nanobubbles. *Langmuir* **2004,** 20, (1), 164-168.
18. Slavchov, R.; Radoev, B.; Stockelhuber, K. W., Equilibrium profile and rupture of wetting film on heterogeneous substrates. *Colloids and Surfaces a-Physicochemical and Engineering Aspects* **2005,** 261, (1-3), 135-140.
19. Sheludko, A., Thin liquid films. *Advances in Colloid and Interface Science* **1967,** 1, (4), 391-464.
20. Jing-Den Chen, J. C. S., Effects of London-van der Waals forces on the thinning of a dimpled liquid film as a small drop or bubble approaches a horizontal solid plane. *Aiche Journal* **1982,** 28, (6), 955-963.
21. Frankel, S. P.; Myseis, K. J., On the "dimpling" during the approach of two interfaces. *The Journal of Physical Chemistry* **1962,** 66, (1), 190-191.
22. C.-Y. Lin, J. C. S., Thinning of a liquid film as a small drop or bubble approaches a solid plane. *Aiche Journal* **1982,** 28, (1), 147-156.

23. Sheludko, A., Exerowa, D., *Koloid-Z.* **1959,** 165.
24. Israelachvili, J., *Intermolecular & Surface Forces, 2nd Edition*. Academic Press INC.: San Diego, 1992.
25. Somasundaran, P.; Healy, T. W.; Fuerstenau, D. W., Surfactant Adsorption at the Solid-Liquid Interface dependence of Mechanism on Chain Length. *The Journal of Physical Chemistry* **1964,** 68, (12), 3562-3566.
26. Zhang, J. H.; Yoon, R. H.; Eriksson, J. C., AFM surface force measurements conducted with silica in C(n)TACl solutions: Effect of chain length on hydrophobic force. *Colloids and Surfaces a-Physicochemical and Engineering Aspects* **2007,** 300, (3), 335-345.
27. Jinhong, Z. Surface forces between silica surfaces in CnTACl solutions and surface free energy characterization of talc Virginia Polytechnic Institute and State University, 2006.

Chapter 4

Conclusion and Future work

4.1 Conclusion

In the present work, the drainage of wetting film on the flat hydrophobic surface hydrophobized by *ex-site* adsorption of potassium amyl xanthate (PAX) on gold surface and *in-site* adsorption of Octadecyltrimethylammonium chloride (C_{18}TACl) on the silica surface is investigated by Thin Film Balance technique. The major findings of the present work are discussed as follows:

(1) Reynolds equation is illustrated to successfully predict the thinning kinetics of wetting film at the barrier ring on the hydrophilic silica surface. By assuming negligible influence from the slippage on the solid/liquid interface, the kinetics curve of wetting film drainage on hydrophobic forces is fitted by Reynolds equation corrected by considering the hydrophobic forces in DLVO theory. Long-range hydrophobic forces are responsible for fast drainage of wetting film on and hydrophobic surface.

(2) The film profile of wetting film on the hydrophilic surface is substantially different from that on the hydrophobic surface. Wetting film on the hydrophilic surface is thinning gradually and stabilized at certain film thickness, while wetting film on the hydrophobic surface ruptures spontaneously with large dimple shape due to the strong attractive forces. The changing film profile on PAX-coated gold surface is symmetric due to the uniform coating of PAX on gold surface. The rupture of wetting film on the silica surface in C_{18}TACl aqueous solution is heterogeneous, probably because of the cluster formation of $C_{18}TA^+$ cationic surfactants on silica surface.

(3) The results obtained in the present work shows that the thinning kinetics of wetting film on the hydrophobic surface is strongly dependent on collector concentration and immersion time. The calculated hydrophobic forces constant K_{132} is correlated to contact angle, which also suggests that the hydrophobic forces are corresponding to the thermodynamic condition for bubble-particle attachment. The presence of electrolyte in solution diminishes the hydrophobic forces between the air bubble and the hydrophobic plates.

(4) The combing rule for determining K_{132} for bubble-particle interaction is firstly illustrated experimentally using the TFB technique. The hydrophobic forces between air bubbles K_{232} in the pure water is extrapolated to the 5.3×10^{-17} J, which is a little larger than the results we reported previous. It suggests that the air bubble is most hydrophobic substance due to the high interfacial tension.

4.2 Future Work

The main objective of present work is to measure the thinning kinetics of wetting film on the hydrophobic surfaces, and to verify the combining rule for flotation. The future work is focus on as follows.

(1) The thinning kinetics of wetting film at the barrier ring in the present work is illustrated to satisfy the Reynolds lubrication approximation. The future work is to predict the whole film profile of wetting film on the hydrophobic surface including the effect from the hydrodynamic forces. Also the effect of slippage on the drainage of wetting film on the hydrophobic surface will be discussed.

(2) In the present work, K_{132} determined from the drainage of wetting film on the gold hydrophobized by *ex-site* adsorption of PAX is used to compare with K_{131} determined using AFM to verify the combining rule. The future work is to investigate the drainage of wetting film on the sulfide mineral surface, which is more related to the real practical flotation. The combining rule needs to be further verified in sulfide mineral flotation and possible theoretical explanation will be discussed.